

- analysis. *Nature* 2008, 454:49–55.
- [7] Makino H, et al.: Mesenchymal to embryonic incomplete transition of human cells by chimeric OCT4/3 (POU5F1) with physiological co-activator EWS. *Exp Cell Res* 2009, 288:2727–2740.
  - [8] Nagata S, et al.: Efficient reprogramming of human and mouse primary extra-embryonic cells to pluripotent stem cells. *Genes Cells* 2009, 14:1395–1404.
  - [9] Saito S, Aburatani S, Horimoto K: Network evaluation from the consistency of the graph structure with the measured data. *BMC Sys Biol* 2008, 2:84.
  - [10] Sridharan R, et al.: Role of the murine reprogramming factors in the induction of pluripotency. *Cell* 2009, 136:364–377.
  - [11] Subramanian A, et al.: Gene set enrichment analysis: A knowledge-based approach for interpreting genome-wide expression profiles. *Proc Natl Acad Sci USA* 2005, 102:15545–15550.
  - [12] Kuno A, et al.: Evanescent-field fluorescence-assisted lectin microarray: a new strategy for glycan profiling. *Nat. Methods* 2005, 2:851–856.
  - [13] Lin T et al.: A chemical platform for improved induction of human iPSCs. *Nat Methods* 2009, 6:805–808.
  - [14] Sumi T, Tsuneyoshi N, Nakatsuji N, Suemori H: Defining early lineage specification of human embryonic stem cells by the orchestrated balance of canonical Wnt/beta-catenin, Activin/Nodal and BMP signaling. *Development* 2008, 135:2969–2979.
  - [15] Eiselleova L, et al.: A complex role for FGF-2 in self-renewal, survival, and adhesion of human embryonic stem cells. *Stem Cells* 2009, 27:1847–1857.
  - [16] Discher DE, Mooney DJ, Zandstra PW: Growth Factors, matrices, and forces combine and control stem cells. *Science* 2009, 26:1673–1677.
  - [17] Yamanaka S: Elite and stochastic models for induced pluripotent stem cell generation. *Nature* 2009, 460:49–52.
  - [18] Satomaa T, et al.: The N-glycome of human embryonic stem cells. *BMC Cell Biol* 2009, 10:42.
  - [19] Levenstein ME, et al.: Secreted proteoglycans directly mediate human embryonic stem cell-basic fibroblast growth factor 2 interactions critical for proliferation. *Stem Cells* 2008, 26:3099–3107.
  - [20] Gabius H-J: Glycans: bioactive signals decoded by lectins. *Biochem Soc Trans* 2008, 36:1491–1496
  - [21] Hashimoto K, et al.: Comprehensive analysis of glycosyltransferases in eukaryotic genomes for structural and functional characterization of glycans. *Carbohydr Res* 2009, 12:881–887.
  - [22] Shevinsky L, Knowles BB, Damjanov I, Solter D: Monoclonal antibody to murine embryos defines a stage-specific embryonic antigen expressed on mouse embryos and human teratocarcinoma cells. *Cell* 1982, 30:697–705.
  - [23] Kannagi R et al.: Stage-specific embryonic antigens (SSEA-3 and -4) are epitopes of a unique globo-series ganglioside isolated from human teratocarcinoma cells. *EMBO J* 1983, 2:2355–2361.
  - [24] Gooi HC, et al.: Stage-specific embryonic antigen involves a1→3 fucosylated type 2 blood group chains. *Nature* 1981, 292:156–158.
  - [25] Bert JE, et al.: The HB-6, CDw75, and CD76 differentiation antigens are unique cell-surface carbohydrate determinants generated by the  $\beta$ -galactoside a2,6-sialyltransferase. *J Cell Biol* 1992, 116:423–435.

## Oncostatin M Renders Epithelial Cell Adhesion Molecule–Positive Liver Cancer Stem Cells Sensitive to 5-Fluorouracil by Inducing Hepatocytic Differentiation

Taro Yamashita, Masao Honda, Kouki Nio, Yasunari Nakamoto, Tatsuya Yamashita, Hiroyuki Takamura, Takashi Tani, Yoh Zen, and Shuichi Kaneko

### Abstract

Recent evidence suggests that a certain type of hepatocellular carcinoma (HCC) is hierarchically organized by a subset of cells with stem cell features (cancer stem cells; CSC). Although normal stem cells and CSCs are considered to share similar self-renewal programs, it remains unclear whether differentiation programs are also maintained in CSCs and effectively used for tumor eradication. In this study, we investigated the effect of oncostatin M (OSM), an interleukin 6–related cytokine known to induce the differentiation of hepatoblasts into hepatocytes, on liver CSCs. OSM receptor expression was detected in the majority of epithelial cell adhesion molecule–positive (EpCAM<sup>+</sup>) HCC with stem/progenitor cell features. OSM treatment resulted in the induction of hepatocytic differentiation of EpCAM<sup>+</sup> HCC cells by inducing signal transducer and activator of transcription 3 activation, as determined by a decrease in stemness-related gene expression, a decrease in EpCAM,  $\alpha$ -fetoprotein and cytokeratin 19 protein expressions, and an increase in albumin protein expression. OSM-treated EpCAM<sup>+</sup> HCC cells showed enhanced cell proliferation with expansion of the EpCAM-negative non-CSC population. Noticeably, combination of OSM treatment with the chemotherapeutic agent 5-fluorouracil (5-FU), which eradicates EpCAM-negative non-CSCs, dramatically increased the number of apoptotic cells *in vitro* and suppressed tumor growth *in vivo* compared with either saline control, OSM, or 5-FU treatment alone. Taken together, our data suggest that OSM could be effectively used for the differentiation and active cell division of dormant EpCAM<sup>+</sup> liver CSCs, and the combination of OSM and conventional chemotherapy with 5-FU efficiently eliminates HCC by targeting both CSCs and non-CSCs. *Cancer Res*; 70(11); 4687–97. ©2010 AACR.

### Introduction

It is widely accepted that cancer is a disease that develops from a normal cell with accumulated genetic/epigenetic changes. Although considered monoclonal in origin, cancer is composed of heterogeneous cellular populations. These heterogeneities are traditionally explained by the clonal evolution of cancer cells through a series of stochastic genetic events (clonal evolution model; ref. 1). In contrast, cancer cells are known to have the capabilities characteristic of stem cells with respect to self-renewal, limitless division, and gen-

eration of heterogeneous cell populations. Recent evidence suggests that tumor cells possess stem cell features (cancer stem cells; CSC) to self-renew and give rise to relatively differentiated cells through asymmetric division, and thereby form heterogeneous populations (CSC model; refs. 2, 3). Accumulating evidence supports the notion that CSCs could generate tumors more efficiently in immunodeficient mice than non-CSCs in the case of leukemia and various solid tumors (4–9), although the origin of CSCs is still a controversial issue.

Worldwide, hepatocellular carcinoma (HCC) is one of the most common malignancies with poor outcome (10). Recent evidence suggests that at least some HCCs are organized by liver CSCs in a hierarchical manner (11). Several markers have been identified as useful for the enrichment of liver CSCs, including side population fraction (12), CD133 (13), CD90 (14), and OV6 (15). We have recently used epithelial cell adhesion molecule (EpCAM) and  $\alpha$ -fetoprotein (AFP) to identify novel prognostic HCC subtypes related to certain developmental stages of human liver lineages (16). Among these, EpCAM-positive (EpCAM<sup>+</sup>) AFP<sup>+</sup> HCC (hepatic stem cell–like HCC) is characterized by young onset of disease, activation of Wnt/ $\beta$ -catenin signaling, and poor prognosis. *EPCAM* is a target gene of Wnt/ $\beta$ -catenin signaling (17), and we previously identified that EpCAM<sup>+</sup> HCC cells from primary HCC

**Authors' Affiliation:** Center for Liver Diseases, Kanazawa University Hospital, Kanazawa, Ishikawa, Japan

**Note:** Supplementary data for this article are available at Cancer Research Online (<http://cancerres.aacrjournals.org>).

**Corresponding Authors:** Taro Yamashita, Department of Gastroenterology, Kanazawa University Graduate School of Medical Science, 13-1 Takara-Machi, Kanazawa, Ishikawa 920-8641, Japan. Phone: 81-76-265-2851; Fax: 81-76-265-4250; E-mail: taroy@m-kanazawa.jp and Shuichi Kaneko, Center for Liver Diseases, Kanazawa University Hospital; Department of Gastroenterology, Kanazawa University Graduate School of Medical Science, 13-1 Takara-Machi, Kanazawa, Ishikawa 920-8641, Japan. Phone: 81-76-265-2230; Fax: 81-76-265-4250; E-mail: skaneko@m-kanazawa.jp.

**doi:** 10.1158/0008-5472.CAN-09-4210

©2010 American Association for Cancer Research.

samples and cell lines have the features of CSCs, at least in the hepatic stem cell-like HCC subtype (18). Thus, EpCAM seems to be a potentially useful marker for the isolation of liver CSCs in hepatic stem cell-like HCC.

CSCs are considered to be resistant to chemotherapy and radiotherapy (19–21), which may be associated with the recurrence of the tumor after treatment. These findings have led to the proposal of “destemming” CSCs, to induce the differentiation of CSCs into non-CSCs or to eradicate CSCs by inhibiting the signaling pathway responsible for self-renewal (22). Recent studies support this proposal and suggest the utility of bone morphogenetic proteins, activated during embryogenesis and required for differentiation of neuronal stem cells, to induce differentiation of brain CSCs and facilitate brain tumor eradication (23, 24). However, it is still debatable whether simple differentiation of CSCs effectively eradicates tumors (25).

Oncostatin M (OSM), an interleukin (IL)-6-related cytokine produced by CD45<sup>+</sup> hematopoietic cells, is known to enhance hepatocytic differentiation of hepatoblasts by inducing the activation of the signal transducer and activator of transcription 3 (STAT3) pathway (26). Although OSM, IL-6, and leukemia-inhibitory factor share STAT3 signaling cascades, OSM is known to exploit the distinct hepatocytic differentiation signaling in an OSM receptor (OSMR)-specific manner (27). In this study, we hypothesized that OSM induces hepatocytic differentiation of liver CSCs through the OSMR signaling pathway. We examined OSMR expression and the effect of OSM in EpCAM<sup>+</sup> HCC in terms of hepatocytic differentiation and antitumor activities.

## Materials and Methods

### Clinical HCC specimens

A total of 107 HCC tissues and adjacent noncancerous liver tissues were obtained from patients who underwent hepatectomy for HCC treatment from 1999 to 2007 in Kanazawa University Hospital. These samples were formalin-fixed and paraffin-embedded, and used for immunohistochemistry. HCC and adjacent noncancerous liver tissues were histologically diagnosed by two pathologists. An additional fresh EpCAM<sup>+</sup> AFP<sup>+</sup> HCC sample was obtained from a surgically resected specimen and immediately used for the preparation of single-cell suspensions and xenotransplantation. All tissue acquisition procedures were approved by the Ethics Committee and the Institutional Review Board of Kanazawa University Hospital. All patients provided written informed consent.

### Cell culture and reagents

HuH1 and HuH7 cells were cultured as previously described (18). A primary HCC tissue was dissected and digested in 1 µg/mL of type 4 collagenase (Sigma-Aldrich Japan K.K.) solution at 37°C for 15 to 30 minutes. Contaminated RBC were lysed with ammonium chloride solution (STEM-CELL Technologies) on ice for 5 minutes. CD45<sup>+</sup> leukocytes and Annexin V<sup>+</sup> apoptotic cells were removed by autoMACS-pro cell separator and magnet beads (Miltenyi Biotec K.K.). EpCAM-positive and -negative cells were enriched by auto-

MACS-pro cell separator and CD326 (EpCAM) MicroBeads (Miltenyi Biotec K.K.). Recombinant OSM was purchased from R&D Systems, Inc. 5-Fluorouracil (5-FU) was obtained from Kyowa Kirin.

### Quantitative reverse transcription-PCR analysis

Total RNA was extracted using TRIzol (Invitrogen) according to the instructions of the manufacturer. The expression of selected genes was determined in triplicate using the 7900 Sequence Detection System (Applied Biosystems). Each sample was normalized relative to β-actin expression. Probes used were *TACSTD1*, Hs00158980\_m1; *AFP*, Hs00173490\_m1; *KRT19*, Hs00761767\_s1; *hTERT*, Hs00162669\_m1; *Bmi1*, Hs00180411\_m1; *POU5F1*, Hs00999632\_g1; *CYP3A4*, Hs00430021\_m1; *OSMR*, Hs00384278\_m1; and *ACTB*, Hs99999903\_m1 (Applied Biosystems).

### Western blotting

Whole cell lysates were prepared using radioimmunoprecipitation assay lysis buffer as described previously (28). Rabbit polyclonal antibodies to STAT3 (Cell Signaling Technology, Inc.), rabbit polyclonal anti-OSMR antibodies H-200 (Santa Cruz Biotechnology), mouse monoclonal anti-phosphorylated STAT3 (Tyr<sup>705</sup>) antibody (3E2; Cell Signaling Technology), and mouse monoclonal anti-β-actin antibody (Sigma-Aldrich) were used. Immune complexes were visualized by enhanced chemiluminescence (Amersham Biosciences, Corp.) as described by the manufacturer.

### Immunohistochemistry and immunofluorescence analyses

Immunohistochemistry was performed using Envision+kits (DAKO) according to the instructions of the manufacturer. Anti-EpCAM monoclonal antibody, VU-ID9 (Oncogene Research Products), was used for detecting EpCAM. Goat anti-OSMR polyclonal antibodies (C-20) were obtained from Santa Cruz Biotechnology. Mouse anti-CYP3A4 polyclonal antibodies (Abnova), mouse anti-cytokeratin (CK) 19 monoclonal antibody (DAKO), and mouse anti-Ki-67 monoclonal antibody MIB-1 (DAKO) were used for detecting CYP3A4, CK19, and Ki-67, respectively. Samples with >5% positive staining in a given area for a particular antibody were considered to be positive. For immunofluorescence analyses, anti-EpCAM antibody (Oncogene Research Products), anti-gp130ST antibodies (Santa Cruz Biotechnology), and anti-phosphorylated STAT3 (Tyr<sup>705</sup>) antibody (3E2; Cell Signaling Technology) were used. Alexa 488 FITC-conjugated anti-mouse IgG or Alexa 568 Texas red-conjugated anti-goat/rabbit IgG (Molecular Probes) were used as secondary antibodies. Confocal fluorescence microscopic analysis was performed essentially as previously described (18).

### Fluorescence-activated cell sorting analyses

Cultured cells were trypsinized, washed, and resuspended in HBSS (Lonza) supplemented with 1% HEPES and 2% fetal bovine serum (FBS). Cells were then incubated with FITC-conjugated anti-EpCAM monoclonal antibody Clone Ber-EP4 (DAKO) on ice for 30 minutes, and analyzed using

a FACSCalibur (BD Biosciences). Intracellular AFP, CK19, and albumin levels were examined using a BD Cytotfix/Cytoperm Fixation/Permeabilization Kit (BD Biosciences), anti-AFP mouse monoclonal antibody (Nichirei Biosciences Inc.), anti-CK19 mouse monoclonal antibody (DAKO), and rabbit polyclonal anti-albumin antibodies (Cell Signaling Technology), respectively.

#### Cell proliferation and colony formation assay

For cell proliferation assays,  $2 \times 10^3$  cells were seeded in 96-well plates and cultured with 1% FBS DMEM (control), 1% DMEM with OSM (100 ng/mL), 5-FU (2  $\mu$ g/mL), or OSM (100 ng/mL) and 5-FU (2  $\mu$ g/mL) for 3 to 7 days without media changes. Cell viability was evaluated in quadruplicate using a CellTiter 96 AQueous kit (Promega). For colony formation assays,  $1 \times 10^3$  cells were harvested in a one-well Culture Slide (BD Biosciences) and cultured with 1% FBS DMEM (control) with or without OSM (100 ng/mL). Culture medium was replaced every 3 days and the colonies were fixed with ice-cold 100% methanol and used for immunofluorescence 10 days after the initiation of treatment.

#### RNA interference

siRNAs specific to OSMR (Silencer Select siRNA S17542) and a control siRNA (Silencer Select Negative Control no. 1) were obtained from Ambion (Applied Biosystems). To each well of a six-well plate,  $2 \times 10^5$  cells were seeded 12 hours before transfection. Transfection was performed using LipofectAMINE 2000 (Invitrogen), according to the instructions of the manufacturer. A total of 100 pmol/L of siRNA duplex was used for each transfection.

#### Apoptosis assay

Cells were cultured in 1% FBS DMEM (control), 1% FBS DMEM with OSM (100 ng/mL), 5-FU (2  $\mu$ g/mL), or OSM (100 ng/mL) and 5-FU (2  $\mu$ g/mL) for 3 days in six-well plates or in culture slides (BD Biosciences). Annexin V binding to cell membranes was visualized using Annexin V-FITC antibodies and a FACSCalibur flow cytometer (BD Biosciences). Activation of caspase 3 was visualized by immunohistochemistry or immunofluorescence using anti-active caspase-3 polyclonal antibodies (Promega), as described by the manufacturer.

#### Animal studies

Six-week-old NOD/SCID mice (NOD/NCrCrl-Prkdc<sup>scid</sup>) were purchased from Charles River Laboratories, Inc. The protocol was approved by the Kanazawa University Animal Care and Use Committee. One million tumor cells were suspended in 200  $\mu$ L of DMEM and Matrigel (1:1), and a s.c. injection was performed. The incidence and size of subcutaneous tumors were recorded. Intratumoral injections of 50  $\mu$ L of PBS (control), OSM (2  $\mu$ g/tumor), 5-FU (250  $\mu$ g/tumor), or OSM (2  $\mu$ g/tumor) and 5-FU (250  $\mu$ g/tumor) were initiated twice weekly 48 days after the injection of tumor cells when the average volume of four tumors in each group had reached 400 mm<sup>3</sup>. For histologic evaluation, tumors were formalin-fixed and paraffin-embedded.

#### Statistical analyses

The association of OSMR expression and clinicopathologic characteristics in HCC was examined using either Mann-Whitney *U* or  $\chi^2$  tests. Student's *t* test was used to compare various test groups assayed by quantitative reverse transcription-PCR analysis. All analyses were performed using GraphPad Prism software.

#### Results

##### Distinct expression of OSMRs in HCC

Before exploring the effect of OSM on HCC, we examined the expression of its receptor, OSMR, in surgically resected HCC and adjacent noncancerous liver tissues by immunohistochemistry. Representative staining of OSMRs in tumor/nontumor tissues is shown in Fig. 1A. In general, cell surface and cytoplasmic immunoreactivity to OSMR were rarely detected in hepatocytes in chronic hepatitis liver (a), but were frequently detected in small hepatocyte-like cells in the stroma or transitional cells in the lobule of cirrhotic liver (b), as indicated by the arrows. Note that immunoreactivity to OSMR was not detected in bile duct epithelia or ductular reactions in which EpCAM<sup>+</sup> hepatic progenitor cells are thought to accumulate (Supplementary Fig. S1), suggesting that OSMRs might be expressed in hepatic progenitor cells committed to hepatocytes. Immunoreactivity to OSMRs was more strongly detected in HCC than in noncancerous liver (c), and the expression was heterogeneous in the tumor. Of note, OSMRs were detected in HCC cells at the invasive front area of the tumor (d) where CSCs are known to invade frequently (arrows).

Immunoreactivity to OSMR antibodies and EpCAM antibodies was detected in 66 (61.7%) and 38 (35.5%) of 107 HCC specimens, respectively. The clinicopathologic characteristics of OSMR<sup>+</sup> and OSMR<sup>-</sup> HCC cases are shown in Table 1. OSMR<sup>+</sup> HCC was characterized by high serum AFP values ( $P = 0.009$ ), poorly differentiated morphology ( $P < 0.0001$ ), and a high frequency of EpCAM<sup>+</sup> HCCs ( $P = 0.024$ ), suggesting that the OSMR is expressed in HCC with stem/progenitor cell features. OSMR<sup>+</sup> HCC was also characterized by young onset of disease and male dominance, although these features did not reach statistical significance ( $P = 0.052$  and  $0.058$ , respectively). OSMR was more frequently detected in EpCAM<sup>+</sup> HCCs (76.3%) than in EpCAM<sup>-</sup> HCCs (53.7%). Expression of OSMR and EpCAM was further investigated by double immunofluorescence analysis, and immunoreactivity to OSMR was detected in both EpCAM<sup>+</sup> normal hepatic progenitors (Fig. 1B) and EpCAM<sup>+</sup> HCC cells (Fig. 1C). These data suggest that although OSMR is more widely expressed than EpCAM in HCC, OSMR is frequently expressed in EpCAM<sup>+</sup> normal hepatic progenitors and liver CSCs.

##### OSM induces hepatocytic differentiation of EpCAM<sup>+</sup> HCC

Because OSMR was expressed in the majority of EpCAM<sup>+</sup> HCCs, we investigated the effect of OSM on EpCAM<sup>+</sup> HCC cell lines. First, we examined the expression of OSMR and its signal transducer glycoprotein 130 (gp130) in EpCAM<sup>+</sup> AFP<sup>+</sup> HCC cell lines HuH1 and HuH7 by immunofluorescence

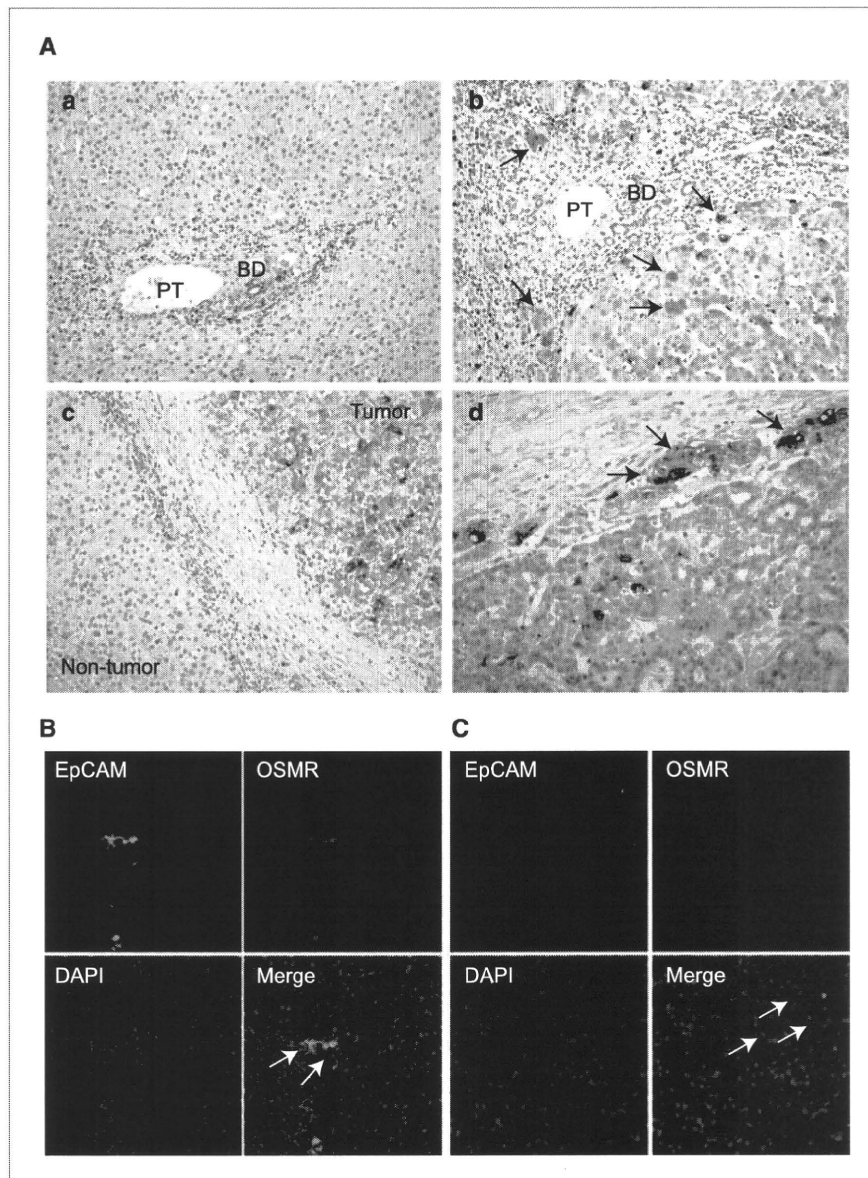


Figure 1. A, representative images of OSMR staining in noncancerous liver tissues and HCC tissues. Immunoreactivity to OSMR was not detected in hepatocytes in chronic hepatitis liver tissue (a) but was detected in a subset of small hepatocyte-like cells in the stroma or transitional cells in the lobule (b, arrows) of cirrhotic liver tissue. OSMR was more abundantly expressed in HCC than in noncancerous liver (c). OSMR<sup>+</sup> cancer cells were disseminated in the invasive front area of the tumor (d, arrows). PT, portal tract; BD, bile duct. B and C, double immunofluorescence analysis of EpCAM (green) and OSMR (red) expression in noncancerous (B) and HCC (C) tissues.

(Fig. 2A). Both gp130 and OSMR protein expressions were detected in these cells, consistent with the immunohistochemical data. Because OSM is known to induce the hepatocytic differentiation of hepatoblasts in a STAT3-dependent manner, we investigated the effect of OSM on phosphorylation of STAT3 in HuH1 and HuH7 cells by immunofluorescence and Western blotting. Incubation of HCC cells for 1 hour with OSM at a concentration of 100 ng/mL resulted in the induction and nuclear accumulation of phosphorylated STAT3 compared with controls (Fig. 2B and C). We examined the effect of OSM on the EpCAM<sup>+</sup> cell population in HuH1 and HuH7 cells. We first labeled HuH1 and HuH7 cells with CD326 (EpCAM) MicroBeads and FITC-conjugated anti-EpCAM

antibodies (Clone Ber-EP4) and performed positive/negative selection using magnetic activated cell sorting to determine the appropriate gating criteria for EpCAM-high (designated as EpCAM<sup>+</sup>) and EpCAM-low/negative (designated as EpCAM<sup>-</sup>) cell population (Fig. 2D, top). It is interesting that OSM treatment (100 ng/mL for 72 hours) diminished the EpCAM<sup>+</sup> cell population from 50.7% to 10.1% in HuH1 and from 55.2% to 28.8% in HuH7 cells when the same constant gating criteria was applied (Fig. 2D, bottom).

We used RNA interference to investigate whether the decrease in EpCAM<sup>+</sup> cells by OSM treatment depends on the expression of OSMR. Transfection of siRNAs specific to *OSMR* (si-OSMR) resulted in the knockdown of target genes

compared with the control (si-Control) in HuH1 and HuH7 cells 48 hours after transfection (Supplementary Fig. S2A). We further confirmed the decrease of OSMR protein expression by immunofluorescence and Western blotting 72 hours after transfection (Supplementary Fig. S2B and C). When we treated these HuH1 and HuH7 cells with OSM (100 ng/mL) for 1 hour, we observed the decrease of phosphorylated STAT3 by *OSMR* gene silencing compared with the control (Supplementary Fig. S2C). Furthermore, OSM-mediated decrease in the number of EpCAM<sup>+</sup> cells was inhibited by *OSMR* gene silencing (Supplementary Fig. S2D), suggesting that OSM exploits the diminution of EpCAM<sup>+</sup> cells through the activation of the OSMR signaling pathway in EpCAM<sup>+</sup> HCC.

We further examined the effect of OSM on hepatocytic differentiation by quantitative reverse transcription-PCR and fluorescence-activated cell sorting (FACS) analyses. OSM treatment in HuH1 cells reduced the expression of hepatic progenitor-related genes including *AFP*, *KRT19* (encoding CK19), and *TERT* (encoding telomerase reverse transcriptase; TERT; Fig. 3A). OSM treatment further reduced the expression of *BM11* and *POU5F1* (encoding Oct4), which is known to be expressed and required for self-renewal in embryonic stem cells. OSM treatment also increased the expression of the hepatocyte marker, *CYP3A4*. Furthermore, OSM treatment reduced AFP<sup>+</sup> and CK19<sup>+</sup> cells and increased albumin<sup>+</sup> cells compared with the untreated controls, as evaluated by the geometric mean of the fluorescence intensities of whole cells analyzed by intracellular FACS (Fig. 3B). Similar results were obtained in HuH7 cells (data not shown) and, taken together, these data suggest that OSM induced the hepatocytic differentiation of EpCAM<sup>+</sup> HCCs.

#### Hepatocytic differentiation of EpCAM<sup>+</sup> HCC by OSM augments cell proliferation

In general, normal stem cells are more quiescent than differentiated cells in terms of cell division. We therefore evaluated the effect of OSM on cell proliferation in HuH1 and HuH7 cells. It is interesting that OSM treatment for 10 days resulted in a larger colony formation following treatment with OSM (100 ng/mL) compared with untreated controls. Of note, the majority of cells comprising these larger colonies were EpCAM<sup>+</sup>, or had low expression levels, whereas a subset of untreated control cells maintained high EpCAM expression (Fig. 3C). Similar results were obtained when cell proliferation was examined using a [3-(4, 5-dimethylthiazol-2-yl)-5-(3-carboxymethoxyphenyl)-2-(4-sulfophenyl)-2H-tetrazolium] tetrazolium assay and Ki-67 labeling index (Fig. 3D). OSM modestly enhanced cell proliferation (top) and increased Ki-67-positive cells (middle and bottom) compared with untreated controls in both HuH1 and HuH7 cells with statistical significance (Fig. 3D).

#### OSM treatment increases chemosensitivity of EpCAM<sup>+</sup> HCC

The abovementioned data imply that although OSM may induce the hepatocytic differentiation of dormant EpCAM<sup>+</sup> liver CSCs, OSM treatment alone might instead enhance cell proliferation through expansion of amplifying differentiated cancer cells *in vitro*, raising the question of efficacy of differentiation therapy in EpCAM<sup>+</sup> HCC. Because rapidly amplifying cells are considered to be more sensitive to chemotherapeutic agents, we investigated the effect of combining OSM treatment with conventional chemotherapy to target both dormant CSCs and amplifying non-CSCs. We have shown that 5-FU treatment

**Table 1.** Clinicopathologic characteristics of OSMR<sup>+</sup> and OSMR<sup>-</sup> HCC cases used for immunohistochemical analyses

Variables	OSMR <sup>+</sup> (n = 66)	OSMR <sup>-</sup> (n = 41)	P*
Age (years, mean ± SE)	62.7 ± 1.3	66.4 ± 1.3	0.052
Sex (male/female)	55/11	27/14	0.058
Etiology (HBV/HCV/other)	25/35/6	8/30/3	0.10
Liver cirrhosis (yes/no)	43/23	26/15	1.0
AFP (ng/mL, mean ± SE)	6,453 ± 5901	1,039 ± 935	0.009
Histologic grade <sup>†</sup>			
I-II	3	16	
II-III	54	20	
III-IV	9	5	<0.0001
Tumor size (<3 cm/>3 cm)	30/36	15/26	0.42
Tumor-node-metastasis classification			
I/II	48	31	
III/IV	18	10	0.82
EpCAM (positive/negative)	29/37	9/32	0.024

\*Mann-Whitney *U* test or  $\chi^2$  test.

<sup>†</sup>Edmondson-Steiner.

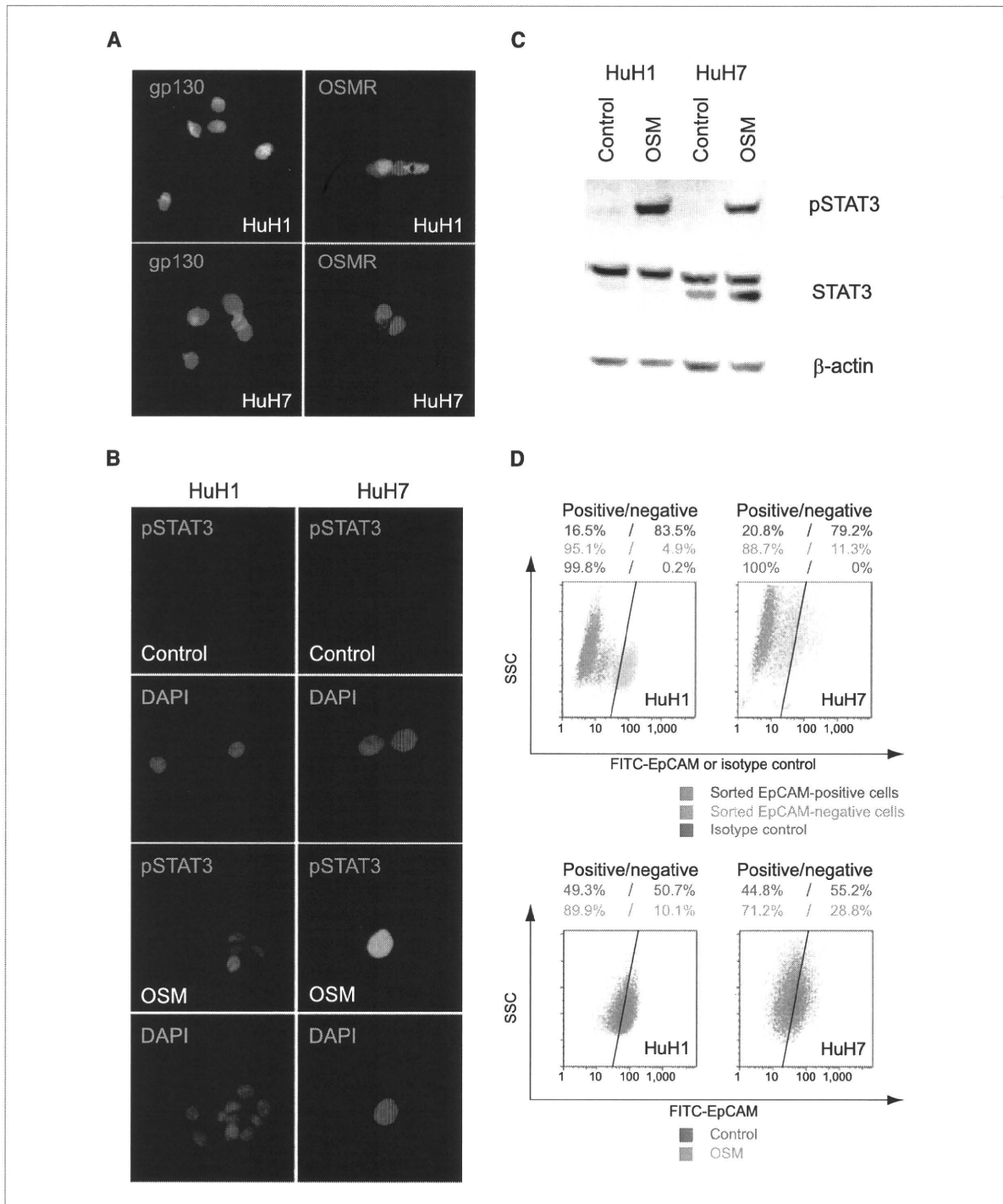


Figure 2. A, immunofluorescence analysis of gp130 and OSMR expression in HuH1 and HuH7 cell lines. B, immunofluorescence analysis of phosphorylated STAT3 expression in HuH1 and HuH7 cell lines stimulated by OSM (100 ng/mL for 1 hour) and controls. C, Western blotting analysis of whole or phosphorylated STAT3 protein expression in HuH1 and HuH7 cells stimulated by OSM (100 ng/mL for 1 hour) and controls. D, FACS analysis of HuH1 and HuH7 cells stained with FITC-conjugated anti-EpCAM antibodies. Top, EpCAM-high (designated as EpCAM<sup>+</sup>; yellow) and EpCAM-low/negative cells (designated as EpCAM<sup>-</sup>; blue) were enriched by magnetic activated cell sorting and labeled with FITC-conjugated anti-EpCAM antibodies or isotype control antibodies. Bottom, cells were cultured in 1% FBS DMEM with (green) or without OSM (100 ng/mL; orange) for 3 days and stained with FITC-conjugated anti-EpCAM antibodies.

alone could diminish EpCAM<sup>-</sup> non-CSCs which results in the enrichment of EpCAM<sup>+</sup> CSCs in HCC (18). We therefore explored the effect of 5-FU in combination with OSM on EpCAM<sup>+</sup> HCC cell proliferation and apoptosis *in vitro*.

When HuH1 and HuH7 cells were treated with OSM alone and cultured for 7 days, cell proliferation was modestly increased compared with untreated controls (Fig. 4A). In contrast, 5-FU treatment clearly inhibited cell proliferation.

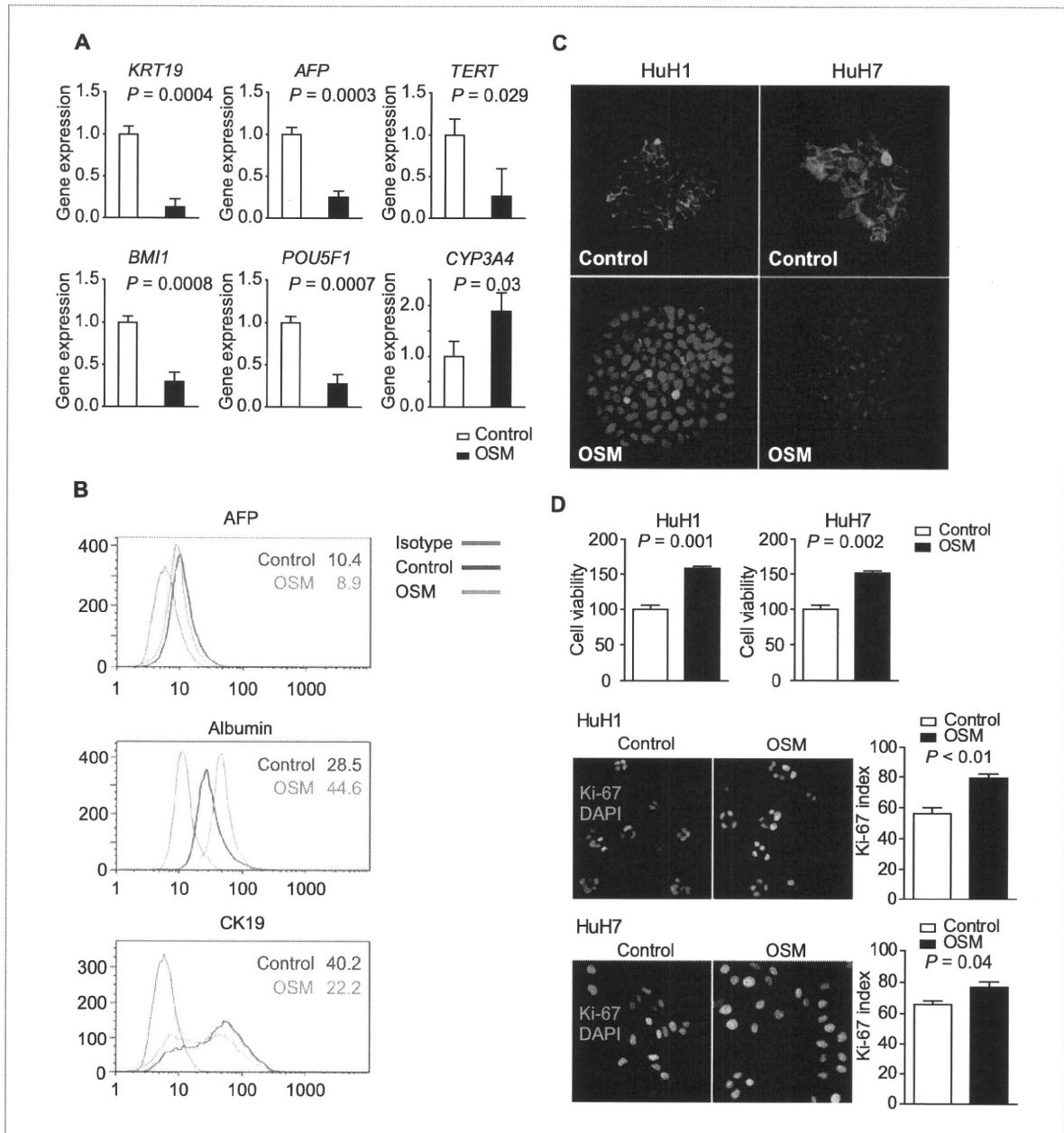


Figure 3. A, quantitative reverse transcription-PCR analysis of HuH1 cells cultured in 1% FBS DMEM with (black columns) or without (white columns) OSM (100 ng/mL) for 3 days. B, intracellular FACS analysis of HuH1 cells cultured in 1% FBS DMEM with (green line) or without (red line) OSM (100 ng/mL) for 3 days. The number in the figure indicates the geometric mean of the fluorescence intensity on a logarithmic scale. C, immunofluorescence analysis of HuH1 and HuH7 cell colonies cultured in 1% FBS DMEM with or without OSM (100 ng/mL) for 10 days. Colonies were fixed with 100% ice-cold methanol and stained with FITC-conjugated anti-EpCAM antibodies. D, top, cell proliferation assay of HuH1 and HuH7 cells cultured in 1% FBS DMEM with (black column) or without (white column) OSM (100 ng/mL) for 3 days. Middle and bottom, immunofluorescence analysis of HuH1 and HuH7 cells cultured in 1% FBS DMEM with or without OSM (100 ng/mL) for 3 days. Cells were fixed with 100% ice-cold methanol and stained with anti-Ki-67 antibodies.

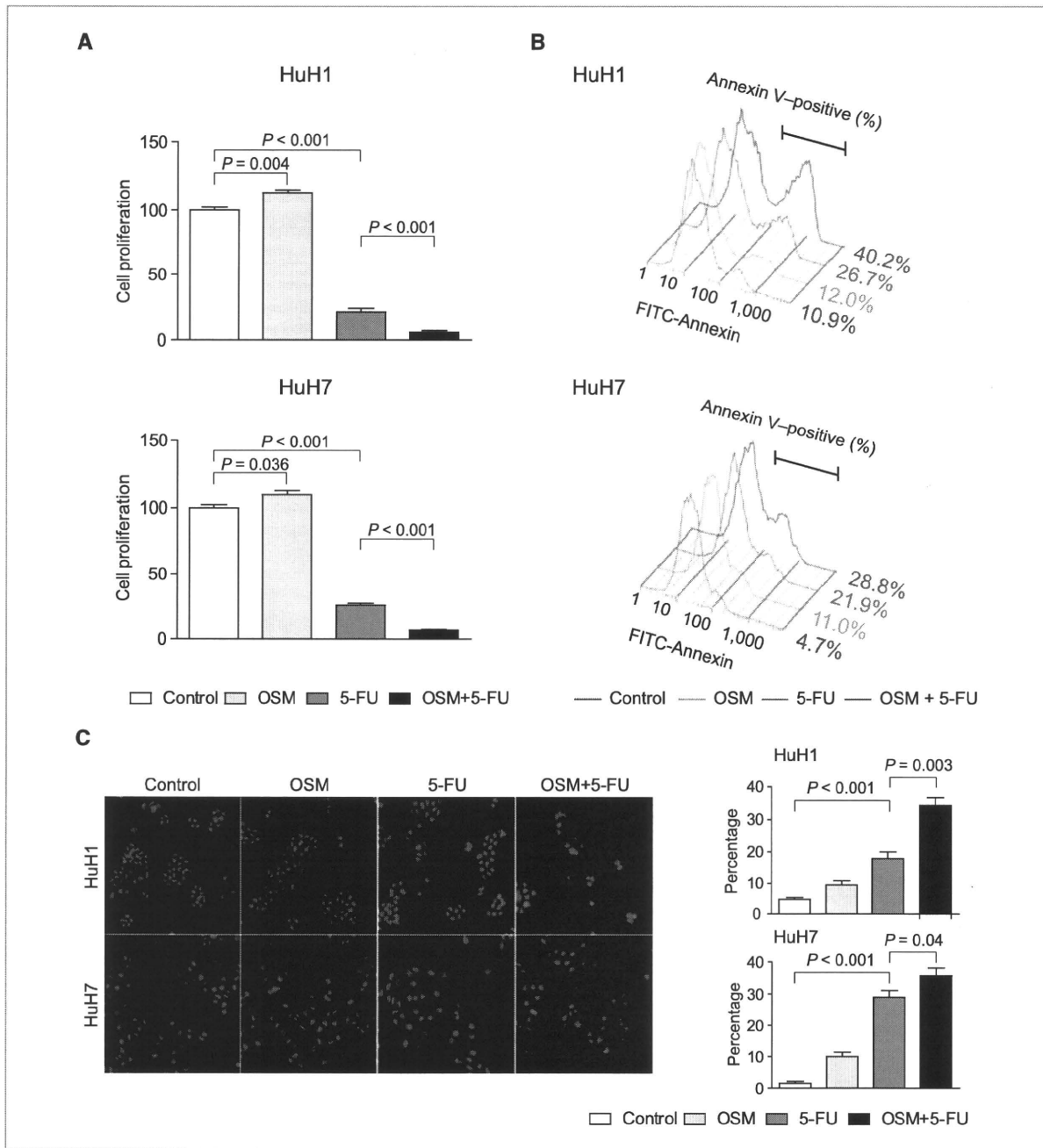


Figure 4. A, cell proliferation assay of HuH1 and HuH7 cells cultured in 1% FBS DMEM with OSM (100 ng/mL; light gray columns), 5-FU (2  $\mu$ g/mL; gray columns), OSM (100 ng/mL) and 5-FU (2  $\mu$ g/mL; black columns), or PBS as control (white columns) for 7 days. B, FACS analysis of HuH1 and HuH7 cells stained with FITC-conjugated anti-Annexin V antibodies. Cells were cultured in 1% FBS DMEM with OSM (100 ng/mL; green line), 5-FU (2  $\mu$ g/mL; blue line), OSM (100 ng/mL) and 5-FU (2  $\mu$ g/mL; red line), or PBS as control (gray line) for 3 days. C, left, immunofluorescence analysis of HuH1 and HuH7 cells stained with anti-active caspase 3 antibodies. Cells were cultured in 1% FBS DMEM with OSM (100 ng/mL), 5-FU (2  $\mu$ g/mL), OSM (100 ng/mL) and 5-FU (2  $\mu$ g/mL), or PBS control for 3 days. Right, bar graphs indicating the percentages of active caspase 3-positive cells.

Noticeably, the combination of OSM and 5-FU effectively suppressed cell proliferation in HuH1 and HuH7 cells (Fig. 4A). We further investigated the effects of OSM and 5-FU on apoptosis, evaluated by Annexin V binding to cell

membranes and the activation of caspase 3 (Fig. 4B and C). Although OSM treatment alone had a small effect on the induction of apoptosis, 5-FU treatment induced Annexin V<sup>+</sup> and activated caspase 3<sup>+</sup> cells more than in the control. The

combination of OSM and 5-FU most strongly induced apoptosis in both HuH1 and HuH7 cells with statistical significance.

Finally, we investigated the effect of OSM on EpCAM<sup>+</sup> HCC *in vivo* using a primary HCC specimen and cell lines. Single-cell suspensions from primary EpCAM<sup>+</sup> HCC cells ( $1 \times 10^6$  cells) were injected into 6-week-old male NOD/SCID mice, and these cells formed subcutaneous tumors 48 days after transplantation. Subsequently, 50  $\mu$ L of PBS, OSM (2  $\mu$ g/tumor), 5-FU (250  $\mu$ g/tumor), or OSM (2  $\mu$ g/tumor) and 5-FU (250  $\mu$ g/tumor) solution were injected directly into each tumor twice a week. Although OSM treatment alone showed weak tumor-suppressive effects, the changes in tumor size showed no significant difference compared with controls (Fig. 5A). Similarly, 5-FU treatment alone showed limited tumor-suppressive effects. However, the combination of OSM with 5-FU showed a marked inhibition of tumor growth compared with PBS control or 5-FU alone ( $P = 0.02$  and  $0.05$ , respectively). Immunohistochemical analysis of xenografted tumors showed that OSM treatment decreased the number of EpCAM<sup>+</sup> or CK19<sup>+</sup> cells and increased CYP3A4<sup>+</sup> cells *in vivo* (Supplementary Fig. S3A and B). FACS analysis of xenografted tumors further confirmed the decrease of EpCAM<sup>+</sup> cell population by OSM treatment *in vivo* (Supplementary Fig. S3C). Immunohistochemical analysis revealed that the combination of OSM with 5-FU strongly induced the activation of caspase 3 compared with PBS control, OSM, or 5-FU (Fig. 5B). Taken together, these data suggest that hepatocytic differentiation of EpCAM<sup>+</sup> HCC cells induced by OSM was the most effective for inhibition of tumor growth *in vivo* when the conventional chemotherapeutic agent 5-FU was coadministered.

## Discussion

A growing body of evidence suggests that there are similarities between normal stem cells and CSCs in terms of self-renewal programs (29). We have recently reported that Wnt/ $\beta$ -catenin signaling augments self-renewal and inhibits the differentiation of EpCAM<sup>+</sup> liver CSCs (18). In the present study, we have shown that the OSM-OSMR signaling pathway is maintained in HCCs with stem/progenitor cell features. OSM induces hepatocytic differentiation and activates cell division in dormant EpCAM<sup>+</sup> liver CSCs (Fig. 5C). Furthermore, we have shown that the combination of OSM and 5-FU effectively inhibits tumor cell growth, revealing the importance of targeting both CSCs and non-CSCs for eradication of the tumor.

OSM is a pleiotropic cytokine that belongs to the IL-6 family which includes IL-6, IL-11, and leukemia-inhibitory factor. These cytokines share the gp130 receptor subunit as a common signal transducer, and activate Janus tyrosine kinases and the STAT3 pathway. However, gp130 forms a heterodimer with a unique partner such as the IL-6 receptor, leukemia-inhibitory factor receptor, or OSMR, thus transducing a certain signaling uniquely induced by each cytokine (30). Of note, OSM is known to activate hepatocytic differentiation programs in hepatoblasts in an OSMR-specific manner (27), and our data showed that OSM could induce

hepatocytic differentiation and active cell proliferation in EpCAM<sup>+</sup> HCC through OSMR signaling.

OSMR is expressed in hepatoblasts in the fetal liver (26). We have found that OSMR is frequently expressed in normal hepatic progenitors but is rarely detected in hepatocytes in adult livers. Interestingly, OSMR<sup>+</sup> HCC was characterized by

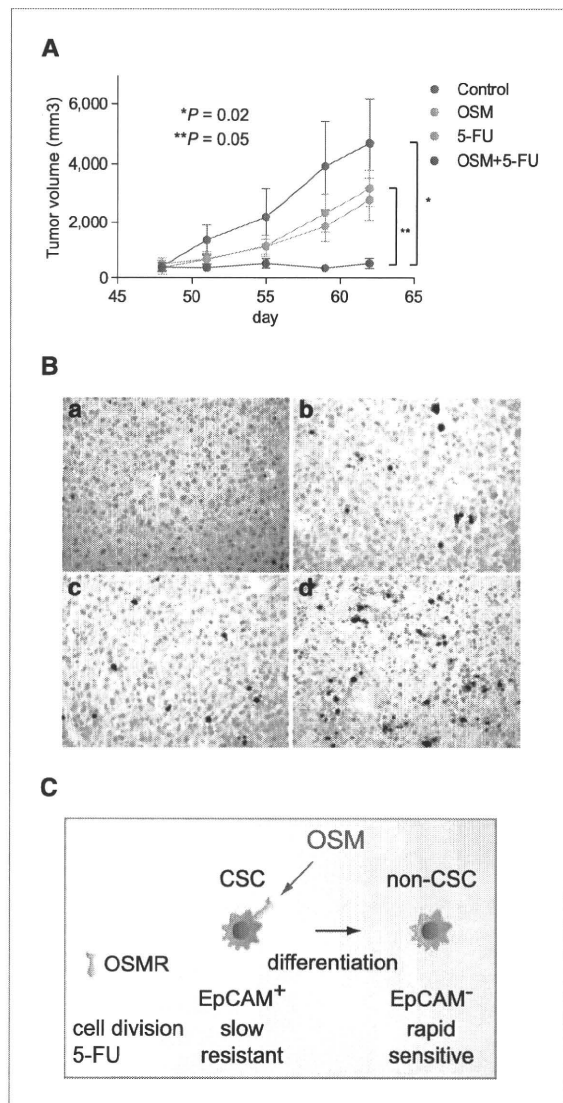


Figure 5. A, effect of PBS, OSM, 5-FU, and OSM plus 5-FU injections on the growth of primary EpCAM<sup>+</sup> AFP<sup>+</sup> HCC xenograft tumors in NOD/SCID mice ( $n = 4$  in each group). Intratumoral injection of 50  $\mu$ L of PBS, OSM (2  $\mu$ g/tumor), 5-FU (250  $\mu$ g/tumor), or OSM (2  $\mu$ g/tumor) and 5-FU (250  $\mu$ g/tumor) was initiated 48 days after transplantation, twice per week. B, representative images of activated caspase 3 staining of xenograft tumors in each treatment group (a, PBS; b, OSM; c, 5-FU; and d, OSM and 5-FU). C, a schematic diagram of the effect of OSM on EpCAM<sup>+</sup> liver CSCs. Dormant EpCAM<sup>+</sup> liver CSCs with OSMR expression respond to OSM and differentiate into rapidly dividing EpCAM<sup>-</sup> non-CSCs that are highly sensitive to 5-FU.

high serum AFP, frequent EpCAM positivity, and poorly differentiated morphology, suggesting that OSMR is more likely expressed in HCC with stem/progenitor cell features (16). Although the regulatory mechanisms of OSMR are still unclear, it is plausible that OSMR expression is regulated by a signaling pathway activated during the process of hepatogenesis. Because gp130 is known to be ubiquitously expressed, regulation of OSM signaling might be largely dependent on the expression status of OSMR in normal and tumor tissues. Recent studies have shown the potential role of methylation of CpG islands located in OSMR promoter in colorectal cancer (31, 32). Clarification of OSMR promoter activity regulation, including CpG methylation, might provide clues for better understanding of hepatocytic differentiation signaling in both normal hepatic stem cells and CSCs.

It has been postulated that both normal stem cells and CSCs are dormant and show slow cell cycles. Consistent with this, CSCs are considered to be more resistant to chemotherapeutic agents than non-CSCs, possibly due to slow cell cycles as well as an increased expression of ATP-binding cassette transporters, robust DNA damage responses, and activated antiapoptotic signaling (20, 33, 34). Therefore, development of an effective strategy by targeting CSC pools together with conventional chemotherapies is essential to eradicate a tumor mass. Two strategies have been investigated to reduce the CSCs population in the tumor; that is, inhibition of self-renewal programs and activation of differentiation programs. We have shown that hepatocytic differentiation of liver CSCs by OSM results in enhanced cell proliferation *in vitro*. We have further shown here that OSM-mediated hepatocytic differentiation of liver CSCs in combination with conventional chemotherapy effectively suppresses HCC growth. It is possible that OSM may boost antitumor activity of 5-FU by "exhausting dormant CSCs" through hepatocytic differentiation and active cell division. It is encouraging that similar success with differentiation therapy has recently been reported in several cancers (24, 35, 36). In addition, HNF4- $\alpha$ -mediated differentiation of HCC cells has recently been reported to be effective for the eradication of HCC (37). However, although the combination of OSM and 5-FU effectively inhibited tumor growth in

our model, we could not observe the shrinkage of the tumor. Thus, induction of CSC's differentiation with eradication of non-CSCs might not be enough for the eradication of the tumor, which might suggest the importance of inhibiting self-renewal as well as stimulating differentiation of CSCs. Because we induced the hepatocytic differentiation of the subcutaneous tumor by local injection of OSM, further rigorous studies are clearly required to assess the effect of OSM on liver CSCs and its utility for differentiation therapy in HCC.

CSCs may acquire resistance against differentiation therapy by additional genetic/epigenetic changes during treatment by clonal evolution, as observed in conventional chemotherapy. Indeed, it has recently been suggested that bone morphogenetic protein-mediated brain CSC differentiation failed in a subset of brain tumors in which bone morphogenetic protein receptor promoters were methylated and silenced (23). Similarly, OSMR silencing by promoter methylation might result in the development of OSM-resistant clones in HCC.

In conclusion, OSMR is expressed in certain types of HCC with stem/progenitor cell features, and OSM induces hepatocytic differentiation and active cell division of OSMR<sup>+</sup> liver CSCs to enhance chemosensitivity to 5-FU. The clinical safety and utility of OSM should be evaluated in the near future.

#### Disclosure of Potential Conflicts of Interest

No potential conflicts of interest were disclosed.

#### Acknowledgments

We thank Masayo Baba and Nami Nishiyama for excellent technical assistance.

#### Grant Support

Ministry of Education, Culture, Sports, Science and Technology, Japan grant-in-aid (no. 20599005).

The costs of publication of this article were defrayed in part by the payment of page charges. This article must therefore be hereby marked *advertisement* in accordance with 18 U.S.C. Section 1734 solely to indicate this fact.

Received 11/17/2009; revised 03/12/2010; accepted 03/31/2010; published OnlineFirst 05/18/2010.

#### References

1. Fialkow PJ. Clonal origin of human tumors. *Biochim Biophys Acta* 1976;458:283–321.
2. Clarke MF, Dick JE, Dirks PB, et al. Cancer stem cells—perspectives on current status and future directions: AACR Workshop on Cancer Stem Cells. *Cancer Res* 2006;66:9339–44.
3. Jordan CT, Guzman ML, Noble M. Cancer stem cells. *N Engl J Med* 2006;355:1253–61.
4. Al-Hajj M, Wicha MS, Benito-Hernandez A, Morrison SJ, Clarke MF. Prospective identification of tumorigenic breast cancer cells. *Proc Natl Acad Sci U S A* 2003;100:3983–8.
5. Bonnet D, Dick JE. Human acute myeloid leukemia is organized as a hierarchy that originates from a primitive hematopoietic cell. *Nat Med* 1997;3:730–7.
6. O'Brien CA, Pollett A, Gallinger S, Dick JE. A human colon cancer cell capable of initiating tumour growth in immunodeficient mice. *Nature* 2007;445:106–10.
7. Ricci-Vitiani L, Lombardi DG, Pilozzi E, et al. Identification and expansion of human colon-cancer-initiating cells. *Nature* 2007;445:111–5.
8. Singh SK, Hawkins C, Clarke ID, et al. Identification of human brain tumour initiating cells. *Nature* 2004;432:396–401.
9. Visvader JE, Lindeman GJ. Cancer stem cells in solid tumours: accumulating evidence and unresolved questions. *Nat Rev Cancer* 2008;8:755–68.
10. El-Serag HB, Rudolph KL. Hepatocellular carcinoma: epidemiology and molecular carcinogenesis. *Gastroenterology* 2007;132:2557–76.
11. Mishra L, Banker T, Murray J, et al. Liver stem cells and hepatocellular carcinoma. *Hepatology* 2009;49:318–29.
12. Chiba T, Kita K, Zheng YW, et al. Side population purified from hepatocellular carcinoma cells harbors cancer stem cell-like properties. *Hepatology* 2006;44:240–51.

13. Ma S, Chan KW, Hu L, et al. Identification and characterization of tumorigenic liver cancer stem/progenitor cells. *Gastroenterology* 2007;132:2542–56.
14. Yang ZF, Ho DW, Ng MN, et al. Significance of CD90+ cancer stem cells in human liver cancer. *Cancer Cell* 2008;13:153–66.
15. Yang W, Yan HX, Chen L, et al. Wnt/ $\beta$ -catenin signaling contributes to activation of normal and tumorigenic liver progenitor cells. *Cancer Res* 2008;68:4287–95.
16. Yamashita T, Forgues M, Wang W, et al. EpCAM and  $\alpha$ -fetoprotein expression defines novel prognostic subtypes of hepatocellular carcinoma. *Cancer Res* 2008;68:1451–61.
17. Yamashita T, Budhu A, Forgues M, Wang XW. Activation of hepatic stem cell marker EpCAM by Wnt/ $\beta$ -catenin signaling in hepatocellular carcinoma. *Cancer Res* 2007;67:10831–9.
18. Yamashita T, Ji J, Budhu A, et al. EpCAM-positive hepatocellular carcinoma cells are tumor-initiating cells with stem/progenitor cell features. *Gastroenterology* 2009;136:1012–24.
19. Boman BM, Huang E. Human colon cancer stem cells: a new paradigm in gastrointestinal oncology. *J Clin Oncol* 2008;26:2828–38.
20. Dean M, Fojo T, Bates S. Tumour stem cells and drug resistance. *Nat Rev Cancer* 2005;5:275–84.
21. Zou GM. Cancer initiating cells or cancer stem cells in the gastrointestinal tract and liver. *J Cell Physiol* 2008;217:598–604.
22. Hill RP, Perris R. "Destemming" cancer stem cells. *J Natl Cancer Inst* 2007;99:1435–40.
23. Lee J, Son MJ, Woolard K, et al. Epigenetic-mediated dysfunction of the bone morphogenetic protein pathway inhibits differentiation of glioblastoma-initiating cells. *Cancer Cell* 2008;13:69–80.
24. Piccirillo SG, Reynolds BA, Zanetti N, et al. Bone morphogenetic proteins inhibit the tumorigenic potential of human brain tumour-initiating cells. *Nature* 2006;444:761–5.
25. Nasr R, Guillemain MC, Ferhi O, et al. Eradication of acute promyelocytic leukemia-initiating cells through PML-RARA degradation. *Nat Med* 2008;14:1333–42.
26. Kamiya A, Kinoshita T, Ito Y, et al. Fetal liver development requires a paracrine action of oncostatin M through the gp130 signal transducer. *EMBO J* 1999;18:2127–36.
27. Kinoshita T, Miyajima A. Cytokine regulation of liver development. *Biochim Biophys Acta* 2002;1592:303–12.
28. Yamashita T, Honda M, Takatori H, et al. Activation of lipogenic pathway correlates with cell proliferation and poor prognosis in hepatocellular carcinoma. *J Hepatol* 2009;50:100–10.
29. Lobo NA, Shimono Y, Qian D, Clarke MF. The biology of cancer stem cells. *Annu Rev Cell Dev Biol* 2007;23:675–99.
30. Heinrich PC, Behrmann I, Haan S, Hermanns HM, Muller-Newen G, Schaper F. Principles of interleukin (IL)-6-type cytokine signalling and its regulation. *Biochem J* 2003;374:1–20.
31. Deng G, Kakar S, Okudaira K, Choi E, Slesinger MH, Kim YS. Unique methylation pattern of oncostatin m receptor gene in cancers of colorectum and other digestive organs. *Clin Cancer Res* 2009;15:1519–26.
32. Kim MS, Louwagie J, Carvalho B, et al. Promoter DNA methylation of oncostatin m receptor- $\beta$  as a novel diagnostic and therapeutic marker in colon cancer. *PLoS One* 2009;4:e6555.
33. Bao S, Wu Q, McLendon RE, et al. Glioma stem cells promote radioresistance by preferential activation of the DNA damage response. *Nature* 2006;444:756–60.
34. Viale A, De Franco F, Orleth A, et al. Cell-cycle restriction limits DNA damage and maintains self-renewal of leukaemia stem cells. *Nature* 2009;457:51–6.
35. Gupta PB, Onder TT, Jiang G, et al. Identification of selective inhibitors of cancer stem cells by high-throughput screening. *Cell* 2009;138:645–59.
36. Sipkins DA. Rendering the leukemia cell susceptible to attack. *N Engl J Med* 2009;361:1307–9.
37. Yin C, Lin Y, Zhang X, et al. Differentiation therapy of hepatocellular carcinoma in mice with recombinant adenovirus carrying hepatocyte nuclear factor-4 $\alpha$  gene. *Hepatology* 2008;48:1528–39.

CLINICAL STUDIES

## dUTP pyrophosphatase expression correlates with a poor prognosis in hepatocellular carcinoma

Hajime Takatori<sup>1</sup>, Taro Yamashita<sup>1</sup>, Masao Honda<sup>1</sup>, Ryuhei Nishino<sup>1</sup>, Kuniaki Arai<sup>1</sup>, Tatsuya Yamashita<sup>1</sup>, Hiroyuki Takamura<sup>2</sup>, Tetsuo Ohta<sup>2</sup>, Yoh Zen<sup>3</sup> and Shuichi Kaneko<sup>1</sup>

1 Department of Gastroenterology, Kanazawa University Graduate School of Medical Science, Ishikawa, Japan

2 Department of Gastroenterologic Surgery, Kanazawa University Graduate School of Medical Science, Ishikawa, Japan

3 Pathology Section, Kanazawa University Hospital, Ishikawa, Japan

### Keywords

dUTP pyrophosphatase – hepatocellular carcinoma – prognosis – serial analysis of gene expression

### Abbreviations

5-FU, 5-fluorouracil; dUTPase, dUTP pyrophosphatase; HCC, hepatocellular carcinoma; IHC, immunohistochemistry; qRT-PCR, quantitative reverse transcription-polymerase chain reaction; SAGE, serial analysis of gene expression.

### Correspondence

Masao Honda, MD, Department of Gastroenterology, Kanazawa University Graduate School of Medical Science, 13-1 Takara-Machi, Kanazawa, Ishikawa 920-8641, Japan  
Tel: +81 76 265 2233  
Fax: +81 76 234 4250  
e-mail: mhonda@m-kanazawa.jp

Received 13 August 2009

Accepted 26 October 2009

DOI:10.1111/j.1478-3223.2009.02177.x

Hepatocellular carcinoma (HCC) is the fifth most common malignancy and the third leading cause of cancer-related death worldwide (1). Several risk factors are responsible for HCC development, including alcoholism, aflatoxin and genetic diseases such as haemochromatosis and  $\alpha$ -1 antitrypsin deficiency; however, the major risk factor is chronic hepatitis owing to hepatitis B virus (HBV) or hepatitis C virus (HCV) infection (2–4). Several treatment options are currently available for HCC management, which include liver transplantation, surgical resection, percutaneous ethanol injection, radiofrequency ablation, transcatheter arterial chemoembolization and systemic or local chemotherapy, and optimal treatment is determined based on tumour stage and liver function (5, 6). However, more than 80% of HCC cases develop advanced HCC after initial treatment (7).

Various chemotherapeutic drugs have been investigated for their antitumour activity in advanced HCC. For example, 5-fluorouracil (5-FU), a thymidylate synthase inhibitor, was the first reported drug studied for the treatment of advanced HCC; however, a median survival rate of 3–5 months has discouraged the further use of 5-FU as a single chemotherapeutic agent (8, 9). Interferon- $\alpha$  (IFN- $\alpha$ ) has been reported to have antitumour activity against advanced HCC, and recent reports have suggested the efficacy of a combination of 5-FU/IFN- $\alpha$  for advanced HCC treatment (10–12), although convincing evidence for improved survival rate remains lacking. A recent study has indicated that 16% of advanced HCC patients responded positively to 5-FU/IFN- $\alpha$  treatment with clear and significant survival benefits compared with stable or progressive disease

### Abstract

**Background:** Hepatocellular carcinoma (HCC) is a malignancy with a poor prognosis, partly owing to the lack of biomarkers that support its classification in line with its malignant nature. To discover a novel molecular marker that is related to the efficacy of treatment for HCC and its biological nature, we performed serial analysis of gene expression (SAGE) in HCC, normal liver and cirrhotic liver tissues. **Methods:** Gene expression profiles of HCC tissues and non-cancerous liver tissues were obtained by SAGE. Suppression of the target gene by RNA interference was used to evaluate its role in HCC *in vitro*. The relation of the identified marker and prognosis was statistically examined in surgically resected HCC patients. **Results:** We identified significant over-expression of *DUT*, which encodes dUTP pyrophosphatase (dUTPase), in HCC tissue, and this was confirmed in about two-thirds of the HCC samples by reverse-transcription polymerase chain reaction ( $n = 20$ ). Suppression of dUTPase expression using short interfering RNAs inhibited cell proliferation and sensitized HuH7 cells to 5-fluorouracil treatment. Nuclear dUTPase expression was observed in 36.6% of surgically resected HCC samples ( $n = 82$ ) evaluated by immunohistochemistry, and its expression was significantly correlated with the histological grades ( $P = 0.0099$ ). Notably, nuclear dUTPase expression correlated with a poor prognosis with statistical significance (HR, 2.47; 95% CI, 1.08–5.66;  $P = 0.032$ ). **Conclusion:** Taken together, these results suggest that nuclear dUTPase may be a good biomarker for predicting prognosis in HCC patients after surgical resection. Development of novel dUTPase inhibitors may facilitate the eradication of HCC.

patients (13). Thus, drug sensitivity appears to be one of the major determinants of the prognosis of advanced HCC patients treated with chemotherapy. Therefore, a hallmark of successful treatment would be the identification of useful biomarkers for determining the survival benefits offered by each treatment strategy.

In this study, we investigated the gene expression profiles of HCCs using serial analysis of gene expression (SAGE) to identify novel molecular markers or targets for the treatment of HCC (14–18). Here, we identified the upregulation of the *DUT* gene that encodes dUTP pyrophosphatase (dUTPase) in HCC. Markedly, HCC with a high nuclear dUTPase expression correlated with a poorly differentiated morphology and a poor prognosis. *DUT* gene knockdown not only suppressed cell proliferation but also sensitized HuH7 cells to low-dose 5-FU.

## Materials and methods

### Samples

All HCC tissues, adjacent non-cancerous liver tissues and normal liver tissues were obtained from 110 patients undergoing a hepatectomy between 1997 and 2006 in Kanazawa University Hospital, Kanazawa, Japan. Five normal liver tissue samples were obtained from patients undergoing surgical resection of the liver for the treatment of metastatic colon cancer. These samples were snap-frozen in liquid nitrogen immediately after resection. One hundred and five HCC and surrounding non-cancerous liver samples were obtained from patients undergoing surgical resection of the liver for HCC treatment, and part of these samples were used for the recent study (19). Three HCC and adjacent non-cancerous liver tissue samples were snap-frozen in liquid nitrogen and later used for SAGE. Twenty HCC tissues and their corresponding non-cancerous liver tissues were also snap-frozen and later used for real-time reverse transcription-polymerase chain reaction (RT-PCR) analysis, as described previously (19). Eighty-two additional HCC samples were formalin-fixed, paraffin-embedded and used for immunohistochemistry (IHC). HCC and adjacent non-cancerous liver tissues were histologically characterized, as reported elsewhere (19).

All strategies used for gene expression analysis as well as tissue acquisition processes were approved by the Ethics Committee and the Institutional Review Board of Kanazawa University Hospital. All procedures and risks were explained verbally to each patient, who then provided written informed consent.

### Serial analysis of gene expression

Total RNA was purified from each homogenized tissue sample using a ToTally RNA extraction kit (Ambion Inc., Austin, TX, USA), and polyadenylated RNA was isolated using a MicroPoly (A) Pure kit (Ambion). A total of 2.5 µg of mRNA per sample was analysed by SAGE (20, 21). SAGE libraries were randomly sequenced at the

Genomic Research Center (Shimadzu-Biotechnology, Kyoto, Japan), and the sequence files were analysed with SAGE 2000 software. The size of each SAGE library was normalized to 300 000 transcripts per library, and the abundance of transcripts was compared with SAGE 2000 software. Monte Carlo simulation was used for selecting genes whose expression levels were significantly different between the two libraries (22). Each SAGE tag was annotated using a gene-mapping website SAGE Genie database (<http://cgap.nci.nih.gov/SAGE/>) and the Source database (<http://smd.stanford.edu/cgi-bin/source/sourceSearch>), as described previously (23).

### Quantitative reverse transcription-polymerase chain reaction

A 1 µg aliquot of each total RNA was reverse-transcribed using SuperScript II reverse-transcriptase (Invitrogen, Carlsbad, CA, USA). Real-time RT-PCR analysis was performed using the ABI PRISM 7700 sequence detection system (Applied Biosystems, Foster City, CA, USA). Using the standard curve method, quantitative PCR was performed in duplicate for each sample–primer set. Each sample was normalized relative to β actin. The assay IDs used were Hs00798995\_s1 for dUTPase and Hs99999903\_m1 for β actin.

### RNA interference targeting *DUT*

Small interfering RNAs (siRNAs) targeting *DUT* or control (scrambled sequence) were synthesized by Dharmacon (Dharmacon Research Inc., Lafayette, CO, USA). The target sequences of *DUT* are 5'-AAGUUGU GAAAACGGACAUUC-3' (*DUT*1) and 5'-CGGACAUU CAGAUAGCGCUTT-3' (*DUT*2). Lipofectamine 2000™ reagent (Invitrogen) was used for transfection according to the manufacturer's instructions.

### Cell proliferation assay, soft agar assay and matrigel invasion assay

Cell proliferation assays were performed using a Cell Titer96 Aqueous kit in quintuplicate (Promega, Madison, WI, USA). For the soft agar assay,  $1 \times 10^4$  cells were suspended in 2 ml of 0.36% agar with growth medium and added in each well of a six-well plate containing a base layer of 0.72% agar. The plates were incubated at 37 °C in a 5% CO<sub>2</sub> incubator for 2 weeks. Matrigel invasion assays were performed using BD BioCoat™ Matrigel Matrix Cell Culture Inserts and Control Inserts (BD Biosciences, San Jose, CA, USA), as described in the manufacturer's instruction. 5-FU was obtained from Kyowa Kirin (Kyowa Kirin, Tokyo, Japan). All experiments were repeated at least twice.

### Immunohistochemistry

Mouse monoclonal anti-dUTPase antibody M01 (Abnova Corporation, Taipei, Taiwan) and mouse antiproliferating

cell nuclear antigen (PCNA) monoclonal antibody PC10 (Calbiochem, San Diego, CA, USA) were used to evaluate the immunoreactivity of HCC and adjacent non-cancerous liver samples using a Dako EnVision+™ kit (Dako, Carpinteria, CA, USA), according to the manufacturer's instruction. Immunoreactivity was evaluated by determining the percentage of cells expressing dUTPase in the examined fields, graded as low (0–50%) or high (> 50%). The PCNA index was evaluated as described previously (19).

### Statistical analysis

Student's *t*-test was used to determine the statistical significance of the differences in cell viability between the two groups. The Mann–Whitney *U*-test was used for the analysis of gene expression between chronic liver disease (CLD) and HCC tissues. The  $\chi^2$ -test was used to evaluate the correlation between clinicopathological characteristics and dUTPase expression status. Univariate and multivariate Cox proportional hazards regression analysis was used to evaluate the association of dUTPase expression and clinicopathological parameters with patient outcome. All statistical analyses were performed using SPSS software (SPSS software package; SPSS Inc., Chicago, IL, USA) and GRAPHPAD PRISM software (GraphPad Software Inc., La Jolla, CA, USA).

## Results

### Gene expression profiling identified the overexpression of *DUT* in hepatocellular carcinoma

To overcome the considerable individual variability of transcriptomic characteristics, we constructed a SAGE library of normal human liver using RNAs derived from five normal liver tissues. In addition, we constructed two SAGE libraries derived from three HCC tissues or corresponding non-cancerous liver tissues from patients who developed HCC with a history of chronic hepatitis C. We detected a total of 226 267 tags corresponding to 45 746 unique tags from these SAGE libraries (supporting information Table S1). After excluding the tags detected only once in each library, we selected 15 333 reliable unique transcripts expressed in at least one of the SAGE libraries to avoid contamination of tags derived from sequence errors. Then, we annotated these transcripts using SAGE Genie database and the Source database to identify the potential subcellular localization of transcripts categorized into eight groups in each SAGE library.

The number of nuclear component-related transcripts was increased in the HCC library compared with the normal liver and non-cancerous liver libraries, whereas the other cellular component-related transcripts did not show this tendency (supporting information Fig. S1). Because nuclear component-related genes may closely correlate with cancer cell proliferation and chemosensitivity (24), we further investigated the expression of nuclear component-related tags in

each library, and identified 10 transcripts associated with nucleotide/nucleoside metabolism that are over-expressed in HCC (Table 1). Using Monte Carlo simulation, we evaluated the significance of differentially expressed transcripts in HCC and corresponding CLD libraries or in HCC and normal liver libraries. We identified a *DUT* gene encoding dUTPase (dUTPase) whose expression was significantly altered ( $P=0.01$ ). We also identified a *TS* gene encoding thymidylate synthase in the list, but the difference did not reach statistical significance.

dUTPase is a phosphatase known to maintain a dUMP pool by catalysing the hydrolysis of dUTP to dUMP, and thus provides a substrate of thymidylate synthase. Its role in HCC is unknown; therefore, we examined *DUT* expression in 20 independent HCC and corresponding non-cancerous liver tissues, and identified significant overexpression of *DUT* in HCC tissue ( $P=0.0015$ ) (Fig. 1A). Moreover, we detected more than a two-fold increase in *DUT* expression in 70% of HBV-related and HCV-related HCC cases (14 of 20 HCCs) compared with the non-cancerous liver tissues (Fig. 1B). We further examined the expression of *DUT* in 238 HCC tissues compared with the non-cancerous liver tissues using publicly available microarray data (GSE5975) (Fig. S2). Consistent with the SAGE data, *DUT* was overexpressed more than two-fold in 121 of 238 HCC tissues (median: 2.03), whereas *TS* was overexpressed more than two-fold in 54 of 238 HCC tissues (median: 1.41) compared with the non-cancerous liver tissues.

### Pivotal role of dUTP pyrophosphatase expression in cell proliferation in hepatocellular carcinoma cell lines

In general, cancer gene signatures discovered by comparison between tumour and non-tumour tissues are more likely to reflect the differences in the control of cell proliferation and growth (25). Accordingly, we investigated the function of dUTPase in cell proliferation in HuH7 cells by *DUT* gene knockdown. *DUT* expression was decreased by 60–70% following the transfection of the siRNA constructs specifically targeting *DUT* 48 h after transfection (*DUT*1 in Fig. 2A and *DUT*2 in Fig. S3A), and cell growth was significantly inhibited compared with the control 72 h after transfection (Fig. 2B and Fig. S3B). Anchorage-independent cell growth was also significantly impaired by *DUT* gene knockdown 14 days after transfection (Fig. 2C). Furthermore, *DUT* gene knockdown decreased the numbers of both migrating and invading cells 72 h after transfection (Fig. 2D and E).

dUTPase is known to be associated with thymidylate synthesis (26), and thus we evaluated the effects of 5-FU, a thymidylate synthase inhibitor, on dUTPase expression in HCC cell lines *in vitro*. When we treated HuH7 cells with low-dose 5-FU (0.25 mg/ml), we could not detect any growth-inhibitory effects (Fig. 2F). Based on this condition, we evaluated the effect of *DUT* gene knockdown on 5-FU sensitivity 72 h after transfection.

**Table 1.** Genes associated with nucleic acid metabolism overexpressed in hepatocellular carcinoma

Tag sequence	Normal liver	Non-cancerous liver	HCC	Fold*	Gene	P-value†
CAGCTCCGCT	0	2	11	5.5	dUTP pyrophosphatase	0.010
AAAGGATAAT	0	0	3	> 3	General transcription factor II H, polypeptide 2	0.127
ACGGTCCAGG	0	0	3	> 3	Cytidine deaminase	0.127
ATGTAGAGTG	0	0	3	> 3	Thymidylate synthase	0.127
TGGGGATTAC	1	0	3	> 3	Zinc ribbon domain containing, 1	0.127
CACCCTGTAC	2	2	6	3	Solute carrier family 29	0.147
GAACGCCTAA	1	1	3	3	Dihydropyrimidinase-like 2	0.308
GCGCTGGTAC	0	1	3	3	2'-5'-oligoadenylate synthetase 3	0.308
CTTAGTGCAA	0	2	4	2	3'-phosphoadenosine 5'-phosphosulphate synthase 2	0.335
TTGTACATC	0	2	3	1.5	Phosphoribosyl pyrophosphatase synthetase-associated protein 1	0.506

\*Fold increase was calculated by dividing the number of tags in HCC by that of tags in non-cancerous liver. To avoid division by 0, a tag value of 1 was used for any tag that was not detectable in one sample.

†Statistical significance of differentially expressed genes between two groups (HCC and non-cancerous liver libraries) was calculated using Monte Carlo simulation.

HCC, hepatocellular carcinoma.

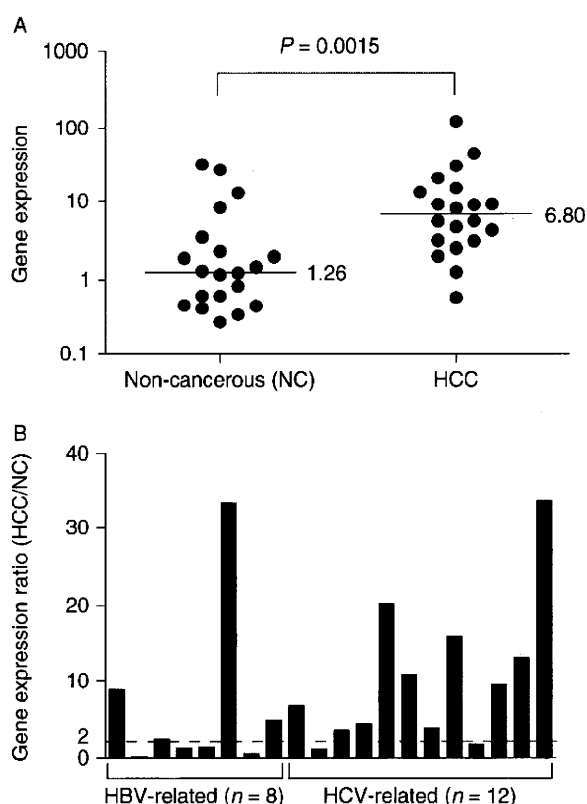


**Fig. 1.** (A) Quantitative reverse transcription-polymerase chain reaction analysis of *DUT* expression in hepatocellular carcinoma (HCC) and corresponding non-cancerous liver tissues. *DUT* was significantly activated in HCC tissues compared with non-cancerous liver tissues ( $P=0.0015$ ). A median value in each group is indicated. (B) *DUT* gene expression ratios of HCC and corresponding non-cancerous liver tissues. Fourteen of 20 HCC tissues expressed *DUT* more than two-fold compared with the background non-cancerous liver tissues. HBV, hepatitis B virus; HCV, hepatitis C virus.

Interestingly, *DUT* gene knockdown not only suppressed cell proliferation but also sensitized HuH7 cells to low-dose 5-FU (Fig. 2F and Fig. S3B). These data suggest that dUTPase overexpression in HCC tissues may be associated with enhanced cell proliferation and 5-FU resistance.

#### Intense dUTP pyrophosphatase expression is correlated with a poor prognosis in hepatocellular carcinoma patients

To characterize the clinicopathological characteristics of dUTPase expression in HCC, we performed IHC using an additional independent HCC cohort. Accordingly, we explored the dUTPase expression in HCC using 82 formalin-fixed paraffin-embedded HCC specimens. All HCC tissues were surgically resected at the Liver Disease Center of Kanazawa University Hospital with full clinical information, and their immunoreactivity to anti-dUTPase antibodies was evaluated by IHC. We noticed that anti-dUTPase antibodies reacted to both nuclear (red arrows) and cytoplasmic (blue arrows) isoforms of dUTPase, as described previously (26) (Fig. 3A and B). We therefore evaluated the nuclear and cytoplasmic expression of dUTPase separately. We stratified HCC tissues and evaluated the dUTPase expression status based on the percentages of dUTPase-positive cells. The frequency of nuclear or cytoplasmic dUTPase-positive cells was highly variable in each HCC tissue, and we defined HCCs with nuclear or cytoplasmic dUTPase expressed in  $\geq 50\%$  of tumour cells as nuclear or cytoplasmic dUTPase-high HCC (Fig. 3C). Nuclear dUTPase overexpression was detected in 36.6% (30 of 82), whereas cytoplasmic dUTPase overexpression was detected in 67.1% (55 of 82) of HCC tissues compared with the corresponding non-cancerous liver tissues

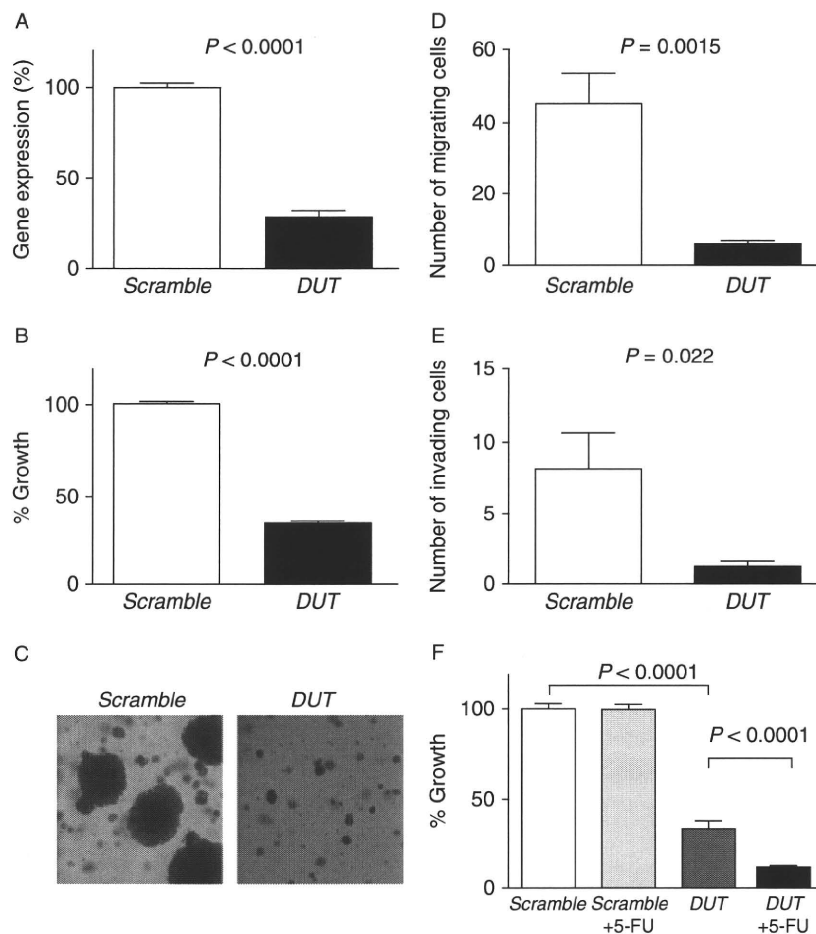


**Fig. 2.** (A) Transfection of small interfering RNAs targeting *DUT* (*DUT1*) decreased *DUT* expression compared with the control (scrambled sequence). Gene expression was evaluated in triplicate 72 h after transfection (mean  $\pm$  SD). (B) *DUT* gene knockdown significantly suppressed cell proliferation ( $P < 0.0001$ ). Cell viability was evaluated in triplicate 72 h after transfection (mean  $\pm$  SD). (C) Soft agar assay. *DUT* gene knockdown suppressed anchorage-independent cell growth. (D and E) Matrigel invasion assay. *DUT* gene knockdown decreased the numbers of both migrating and invading cells. Experiments were performed in triplicate (mean  $\pm$  SD). (F) *DUT* gene knockdown sensitized HuH7 cells to low-dose 5-fluorouracil (5-FU) (0.25  $\mu$ g/ml), which had no effect on the cell proliferation in the control (mean  $\pm$  SD).

(Table 2). In general, non-cancerous hepatocytes rarely expressed nuclear dUTPase (Fig. 3A).

We investigated the clinicopathological characteristics of nuclear or cytoplasmic dUTPase in low/high HCC cases (Table 2). The expression status of nuclear dUTPase showed no correlation with age, gender, virus, presence of cirrhosis,  $\alpha$ -fetoprotein value, tumour size and TNM stages. However, nuclear dUTPase expression was significantly correlated with the histological grades of HCC ( $P = 0.0099$ ), and high frequencies of nuclear dUTPase-positive cells were associated with poorly differentiated cell morphology in the HCC tissue. In contrast, cytoplasmic dUTPase expression was not correlated with the histological grades of HCC ( $P = 0.077$ ). We examined the cell proliferation of these HCC samples by PCNA staining, and PCNA indexes were significantly higher in nuclear dUTPase high HCC than low HCC with statistical significance ( $P = 0.01$ ) (Fig. S4).

We further investigated the prognostic significance of dUTPase expression in HCC. Strikingly, high nuclear dUTPase expression in HCC tissue correlated with a poor survival outcome compared with low nuclear dUTPase expression ( $P = 0.0036$ ), whereas high cytoplasmic dUTPase expression had little effects when evaluated by recurrence-free survival (Fig. 3D). Furthermore, univariate Cox regression analysis showed a significant correlation between high nuclear dUTPase expression and a high risk of mortality (HR, 2.47; 95% CI, 1.08–5.66;  $P = 0.032$ ; Table 3). By multivariate Cox regression analysis, TNM stage (HR, 2.75; 95% CI, 1.11–6.79;  $P = 0.027$ ) and nuclear dUTPase (HR, 2.61; 95% CI, 1.13–6.05;  $P = 0.024$ ) were independent prognostic factors associated with a high risk of mortality, and other clinicopathological features did not add independent prognostic information. These data indicate a significant correlation between the malignant potential of

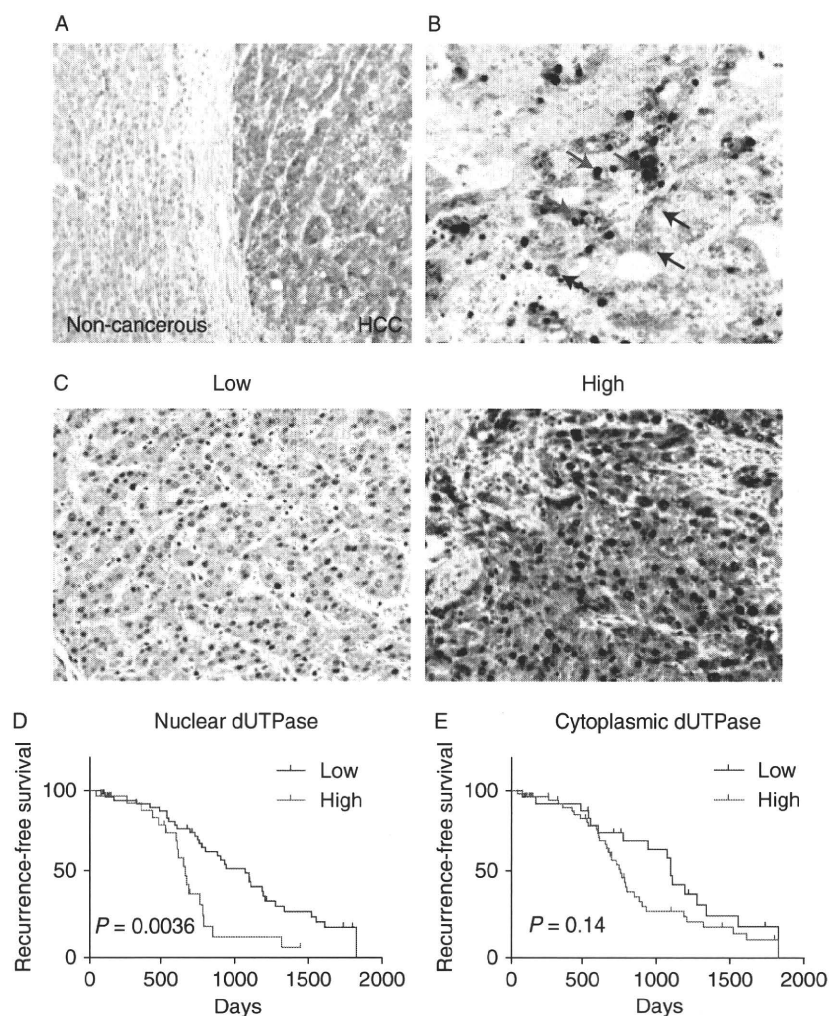


**Fig. 3.** Immunohistochemistry analysis of dUTP pyrophosphatase (dUTPase) expression in hepatocellular carcinoma (HCC). (A) A representative photomicrograph of dUTPase staining in an HCC and adjacent non-cancerous liver tissue. (B) A representative photomicrograph of dUTPase staining in an HCC. Both nuclear (red arrows) and cytoplasmic (blue arrows) forms of dUTPase were detected. (C) Representative photomicrographs of HCC tissues with low (0–50%) and high ( $\geq 50\%$ ) frequencies of nuclear and cytoplasmic dUTPase-positive cells. (D and E) Kaplan–Meier survival analysis of HCC tissues with nuclear (D) or cytoplasmic (E) dUTPase expression. High percentages of nuclear dUTPase-positive tumour cells significantly correlated with poor clinical outcome in recurrence-free survival.

HCC and nuclear dUTPase expression, implicating the potential effectiveness of nuclear dUTPase level as a biomarker for predicting the survival of HCC patients after surgical resection.

### Discussion

Here, using a global gene expression profiling approach (18), we have identified the activation of the nucleotide/nucleoside metabolism-related gene *DUT* (encoding dUTPase) in HCC. Notably, an intense dUTPase expression was detected in a subset of HCC with a poor prognosis. To the best of our knowledge, this is the first

report describing the correlation between dUTPase activation and poor survival outcome in HCC patients.

In normal cells, dUTPase is known to catalyse the hydrolysis of dUTP to dUMP in order to maintain the dUMP pool at a certain level for thymidylate synthesis (26). Interestingly, dUTPase mutations in *Escherichia coli* increased dUTP levels, leading to dUTP misincorporation into DNA during replication, which resulted in DNA fragmentation and apoptosis (27). Furthermore, introduction of *E. coli* dUTPase into human tumour cells resulted in the induction of resistance to fluorodeoxyuridine cytotoxicity (28), suggesting a pivotal role of dUTPase in the prevention of DNA damage. Thus, dUTPase activation in the nucleus appears to be critical

**Table 2.** Clinicopathological characteristics and dUTP pyrophosphatase expression in hepatocellular carcinoma (*n* = 82)

dUTPase expression (nuclear)	Low ( <i>n</i> = 52)	High ( <i>n</i> = 30)	<i>P</i> -value
Age (< 60 years/≥ 60 years)	19/33	8/22	0.36
Sex (male/female)	36/16	23/7	0.47
Virus (HBV/HCV/B+C/NBNC)	15/33/1/3	10/20/0/0	0.48
Cirrhosis (yes/no)	33/19	22/8	0.36
AFP (< 20 ng/ml/≥ 20 ng/ml)	32/20	15/15	0.31
Histological grade*			
I–II	14	3	
II–III	36	20	
III–IV	2	7	0.0099
Tumour size (< 3 cm/≥ 3 cm)	31/21	19/11	0.74
TNM classification† (I, II/III, IV)	43/9	25/5	0.94

dUTPase expression (cytoplasmic)	Low ( <i>n</i> = 27)	High ( <i>n</i> = 55)	<i>P</i> -value
Age (< 60 years/≥ 60 years)	10/17	17/38	0.58
Sex (male/female)	19/8	40/15	0.82
Virus (HBV/HCV/B+C/NBNC)	8/17/1/1	17/36/0/2	0.56
Cirrhosis (yes/no)	17/10	38/17	0.58
AFP (< 20 ng/ml/≥ 20 ng/ml)	16/11	31/24	0.80
Histological grade*			
I–II	7	10	
II–III	20	36	
III–IV	0	9	0.077
Tumour size (< 3 cm/≥ 3 cm)	17/10	33/22	0.80
TNM classification† (I, II/III, IV)	21/6	47/8	0.39

\*Edmondson–Steiner grades.

†UICC TNM classification of liver cancer, 6th edition (2002).

AFP, α-fetoprotein; dUTPase, dUTP pyrophosphatase; HBV, hepatitis B virus; HCV, hepatitis C virus.

for preventing DNA damage possibly at the S phase. Specifically, this activation may prevent dUTP misincorporation in various cancers and thus avert DNA damage and apoptosis induction. Indeed, dUTPase activation has recently been reported in colorectal and brain cancer (29, 30), and dUTPase accumulation might correlate with 5-FU-based chemotherapy resistance and poor prognosis in colorectal cancer (26).

If dUTPase activation plays a central role in the development of resistance to thymidylate synthase inhibitors in order to prevent a DNA damage response, dUTPase inhibition may facilitate the eradication of cancer cells by sensitizing these cells to such inhibitors. Indeed, a recent study suggested a drastic sensitization of colon cancer cells to 5-FU by siRNAs-mediated dUTPase suppression (31, 32), which is consistent with our current observation. Because all HCC samples used in this study were surgically resected, we could not evaluate the effect of dUTPase expression on clinical HCC patients' outcome in relation to chemosensitivity to thymidylate synthase inhibitors. Nevertheless, intense nuclear dUTPase expression may be a good biomarker

**Table 3.** Cox regression analysis of recurrence-free survival rate relative to dUTP pyrophosphatase expression and clinicopathological parameters (*n* = 82)

Variables ( <i>n</i> )	Univariate		Multivariate	
	HR (95% CI)	<i>P</i> -value	HR (95% CI)	<i>P</i> -value
Child–Pugh				
A	1			
B	1.73 (0.50–5.97)	0.38		
Tumour size				
< 3 cm ( <i>n</i> = 50)	1			
≥ 3 cm ( <i>n</i> = 32)	1.58 (0.69–3.63)	0.28		
TNM stage*				
I, II ( <i>n</i> = 68)	1		1	
III, IV ( <i>n</i> = 14)	2.57 (1.05–6.29)	0.039	2.75 (1.11–6.79)	0.027
Serum AFP				
< 20 ng/ml ( <i>n</i> = 49)	1			
≥ 20 ng/ml ( <i>n</i> = 38)	1.54 (0.66–3.56)	0.31		
Microvascular invasion				
No	1			
Yes	1.98 (0.89–4.44)	0.095		
BCLC stage				
A	1			
B/C	2.16 (0.93–5.00)	0.07		
Cytoplasmic dUTPase				
Low ( <i>n</i> = 27)	1			
High ( <i>n</i> = 55)	1.15 (0.50–2.62)	0.73		
Nuclear dUTPase				
Low ( <i>n</i> = 52)	1		1	
High ( <i>n</i> = 30)	2.47 (1.08–5.66)	0.032	2.61 (1.13–6.05)	0.024

\*UICC TNM classification of liver cancer, 6th edition (2002).

AFP, α-fetoprotein; CI, confidence intervals; dUTPase, dUTP pyrophosphatase; HR, hazard ratio.

for predicting the response to thymidylate synthase inhibitors, and its usefulness should be further evaluated in the future.

In conclusion, comprehensive gene expression profiling shed new light on the role of dUTPase in HCC. Nuclear dUTPase accumulation is potentially a good biomarker for predicting poor prognosis in HCC patients, and the development of a dUTPase inhibitor may promote the possibility of tumour eradication in HCC patients.

### Acknowledgements

The authors would like to thank Ms Masayo Baba and Nami Nishiyama for technical assistance. This research was supported in part by a Grant-in-Aid for Special Purposes from the Ministry of Education, Culture, Sports, Science and Technology, Japan (no. 20599005).

**Grant support:** Grant-in-Aid for Special Purposes from the Ministry of Education, Culture, Sports, Science and Technology, Japan (no. 20599005).

## References

- Parkin DM, Bray F, Ferlay J, Pisani P. Global cancer statistics, 2002. *CA Cancer J Clin* 2005; **55**: 74–108.
- El-Serag HB, Rudolph KL. Hepatocellular carcinoma: epidemiology and molecular carcinogenesis. *Gastroenterology* 2007; **132**: 2557–76.
- Farazi PA, Depinho RA. Hepatocellular carcinoma pathogenesis: from genes to environment. *Nat Rev Cancer* 2006; **6**: 674–87.
- Roessler S, Budhu A, Wang XW. Future of molecular profiling of human hepatocellular carcinoma. *Future Oncol* 2007; **3**: 429–39.
- El-Serag HB, Marrero JA, Rudolph L, Reddy KR. Diagnosis and treatment of hepatocellular carcinoma. *Gastroenterology* 2008; **134**: 1752–63.
- Llovet JM, Bruix J. Novel advancements in the management of hepatocellular carcinoma in 2008. *J Hepatol* 2008; **48**(Suppl. 1): S20–37.
- Poon RT, Fan ST, Lo CM, Liu CL, Wong J. Long-term survival and pattern of recurrence after resection of small hepatocellular carcinoma in patients with preserved liver function: implications for a strategy of salvage transplantation. *Ann Surg* 2002; **235**: 373–82.
- Friedman MA. Primary hepatocellular cancer—present results and future prospects. *Int J Radiat Oncol Biol Phys* 1983; **9**: 1841–50.
- Lin DY, Lin SM, Liaw YF. Non-surgical treatment of hepatocellular carcinoma. *J Gastroenterol Hepatol* 1997; **12**: S319–28.
- Nagano H, Miyamoto A, Wada H, *et al.* Interferon-alpha and 5-fluorouracil combination therapy after palliative hepatic resection in patients with advanced hepatocellular carcinoma, portal venous tumor thrombus in the major trunk, and multiple nodules. *Cancer* 2007; **110**: 2493–501.
- Patt YZ, Hassan MM, Lozano RD, *et al.* Phase II trial of systemic continuous fluorouracil and subcutaneous recombinant interferon alfa-2b for treatment of hepatocellular carcinoma. *J Clin Oncol* 2003; **21**: 421–7.
- Urabe T, Kaneko S, Matsushita E, Unoura M, Kobayashi K. Clinical pilot study of intrahepatic arterial chemotherapy with methotrexate, 5-fluorouracil, cisplatin and subcutaneous interferon-alpha-2b for patients with locally advanced hepatocellular carcinoma. *Oncology* 1998; **55**: 39–47.
- Obi S, Yoshida H, Toune R, *et al.* Combination therapy of intraarterial 5-fluorouracil and systemic interferon-alpha for advanced hepatocellular carcinoma with portal venous invasion. *Cancer* 2006; **106**: 1990–7.
- Honda M, Yamashita T, Ueda T, *et al.* Different signaling pathways in the livers of patients with chronic hepatitis B or chronic hepatitis C. *Hepatology* 2006; **44**: 1122–38.
- Nishino R, Honda M, Yamashita T, *et al.* Identification of novel candidate tumour marker genes for intrahepatic cholangiocarcinoma. *J Hepatol* 2008; **49**: 207–16.
- Yamashita T, Honda M, Takatori H, *et al.* Genome-wide transcriptome mapping analysis identifies organ-specific gene expression patterns along human chromosomes. *Genomics* 2004; **84**: 867–75.
- Yamashita T, Kaneko S, Hashimoto S, *et al.* Serial analysis of gene expression in chronic hepatitis C and hepatocellular carcinoma. *Biochem Biophys Res Commun* 2001; **282**: 647–54.
- Yamashita T, Honda M, Kaneko S. Application of serial analysis of gene expression in cancer research. *Curr Pharm Biotechnol* 2008; **9**: 375–82.
- Yamashita T, Honda M, Takatori H, *et al.* Activation of lipogenic pathway correlates with cell proliferation and poor prognosis in hepatocellular carcinoma. *J Hepatol* 2009; **50**: 100–10.
- Velculescu VE, Zhang L, Vogelstein B, Kinzler KW. Serial analysis of gene expression. *Science* 1995; **270**: 484–7.
- Yamashita T, Hashimoto S, Kaneko S, *et al.* Comprehensive gene expression profile of a normal human liver. *Biochem Biophys Res Commun* 2000; **269**: 110–6.
- Polyak K, Xia Y, Zweier JL, Kinzler KW, Vogelstein B. A model for p53-induced apoptosis. *Nature* 1997; **389**: 300–5.
- Misu H, Takamura T, Matsuzawa N, *et al.* Genes involved in oxidative phosphorylation are coordinately upregulated with fasting hyperglycaemia in livers of patients with type 2 diabetes. *Diabetologia* 2007; **50**: 268–77.
- Longley DB, Harkin DP, Johnston PG. 5-fluorouracil: mechanisms of action and clinical strategies. *Nat Rev Cancer* 2003; **3**: 330–8.
- Whitfield ML, George LK, Grant GD, Perou CM. Common markers of proliferation. *Nat Rev Cancer* 2006; **6**: 99–106.
- Ladner RD, Lynch FJ, Groshen S, *et al.* dUTP nucleotidohydrolase isoform expression in normal and neoplastic tissues: association with survival and response to 5-fluorouracil in colorectal cancer. *Cancer Res* 2000; **60**: 3493–503.
- El-Hajj HH, Zhang H, Weiss B. Lethality of a dut (deoxyuridine triphosphatase) mutation in *Escherichia coli*. *J Bacteriol* 1988; **170**: 1069–75.
- Canman CE, Radany EH, Parsels LA, *et al.* Induction of resistance to fluorodeoxyuridine cytotoxicity and DNA damage in human tumor cells by expression of *Escherichia coli* deoxyuridinetriphosphatase. *Cancer Res* 1994; **54**: 2296–8.
- Fleischmann J, Kremmer E, Muller S, *et al.* Expression of deoxyuridine triphosphatase (dUTPase) in colorectal tumours. *Int J Cancer* 1999; **84**: 614–7.
- Romeike BF, Bockeler A, Kremmer E, *et al.* Immunohistochemical detection of dUTPase in intracranial tumors. *Pathol Res Pract* 2005; **201**: 727–32.
- Koehler SE, Ladner RD. Small interfering RNA-mediated suppression of dUTPase sensitizes cancer cell lines to thymidylate synthase inhibition. *Mol Pharmacol* 2004; **66**: 620–6.